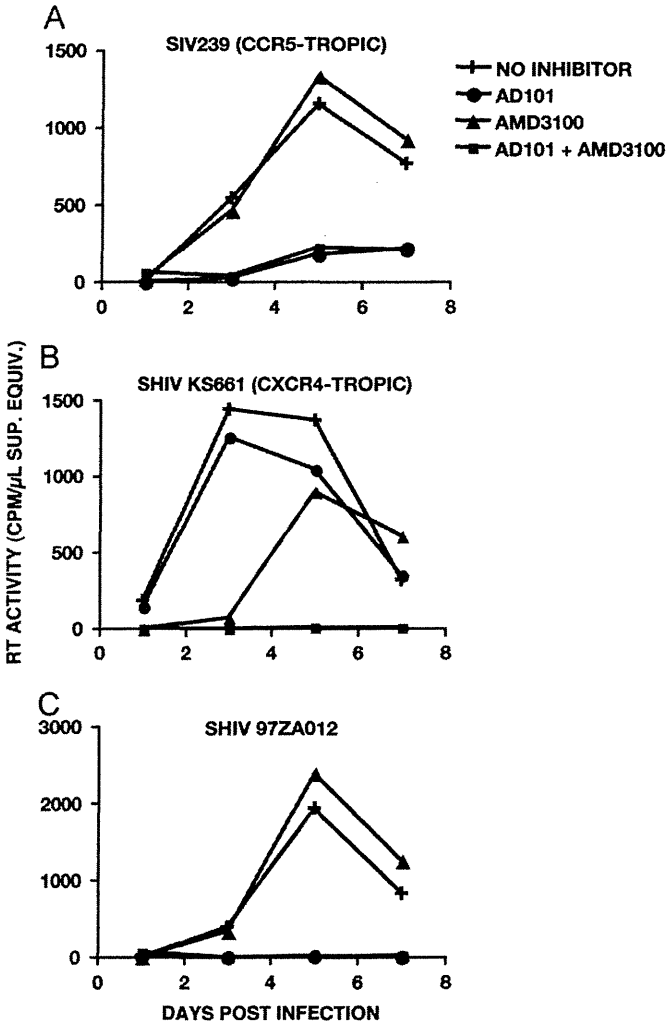

Fig. 5. Co-receptor usage of SHIV 97ZA012. SHIV 97ZA012, along with CCR5-tropic SIV239 and predominantly CXCR4-tropic SHIV KS661, was inoculated into RhPBMCs in the presence of small-molecule co-receptor inhibitor(s) (5 μM), and replication was assessed by reverse transcriptase activity in the culture supernatant for 7 days. The following compounds were utilized as co-receptor inhibitors: AMD3100 for anti-CXCR4 inhibitor and AD101 for anti-CCR5 inhibitor, which was kindly provided by Dr. Julie Strizki, Schering-Plough Research Institute, Kenilworth, NJ.

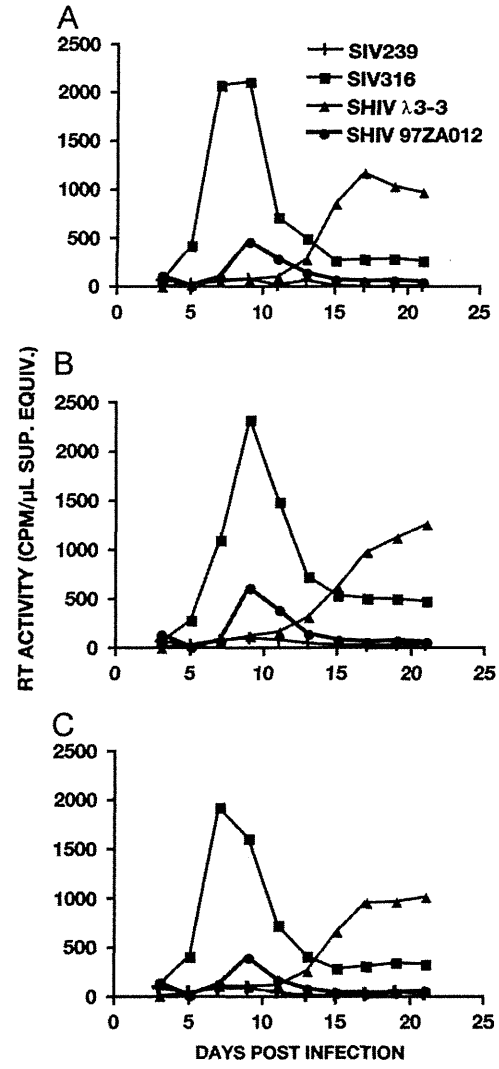

Fig. 6. Replication of SHIV 97ZA012 in primary rhesus alveolar macrophages (RhAMs). SHIV 97ZA012, along with macrophage-tropic SIV316 and SHIV λ3-3 and non-macrophage-tropic SIV239, was inoculated into primary RhAMs, and its replication was monitored for 3 weeks. RhAMs were prepared from three animals independently (A–C). Virus replication was assessed by reverse transcriptase activity in the culture supernatant.

the culture supernatant (Fig. 6). Overall, the viruses exhibited consistent replication profiles among cell cultures prepared from different individuals (Fig. 6A–C). SIV316, a macrophage-tropic variant of SIV239 (Desrosiers et al., 1991), replicated to the highest titers among the viruses, reaching a peak around days 7–9 post-infection (2000–2500 cpm/μl). SHIV λ3-3, a macrophage-tropic SHIV (Igarashi et al., 2007), exhibited a delayed replication profile and reached titers of >1000 cpm/μl after 17 days post-infection. In contrast, SIV239, which is reportedly incapable of replicating in cells of this type (Mori et al., 1993), produced no measurable RT activity in the supernatant during the observation period. Under this condition, SHIV 97ZA012 replicated productively, although not as robustly as SIV316 or SHIV λ3-3, and reached peak virus replication on day 9 post-infection (400–600 cpm/μl). Based on these results, we concluded that SHIV 97ZA012 is macrophage tropic.

Experimental infection of rhesus macaques with SHIV 97ZA012

Biological properties of the newly generated SHIV 97ZA012 revealed in the study, including CCR5 utilization, a robust replication profile in RhPBMCs, and infectiousness in primary macrophages, justified experimental infection of monkeys with the virus. Prior to the infection, we prepared an ample volume of animal challenge stock of the virus by inoculating SHIV 97ZA012 seed to RhPBMCs. Culture supernatant was collected daily and assessed for virus replication by RT activity. Fractions of culture supernatant collected on days 8 and 9 that exhibited the highest RT activities (2450 and 2550 cpm/μl supernatant equivalent) were combined, filtered through a 0.45-μm membrane, divided into aliquots designated SHIV 97ZA012 animal challenge stock, and stored in liquid nitrogen. The infectious titer of the virus stock was 1.51×10^4 $TCID_{50}$/ml, and retention of its preference for CCR5 as an entry co-receptor was verified (data not shown).

The animal challenge stock of SHIV 97ZA012, 1×10^5 $TCID_{50}$, was intravenously inoculated into each of three rhesus macaques. Virus replication was monitored by viral RNA load in plasma samples that were collected periodically (Fig. 7). The virus replicated to substantially high titers in all three animals, reaching an initial peak of 1.03×10^8 copies/ml for MM533, 4.52×10^6 copies/ml for MM535, and 1.83×10^8 copies/ml for MM536 at week 1.1 (day 8) post-inoculation (Fig. 7A). After the initial peak,

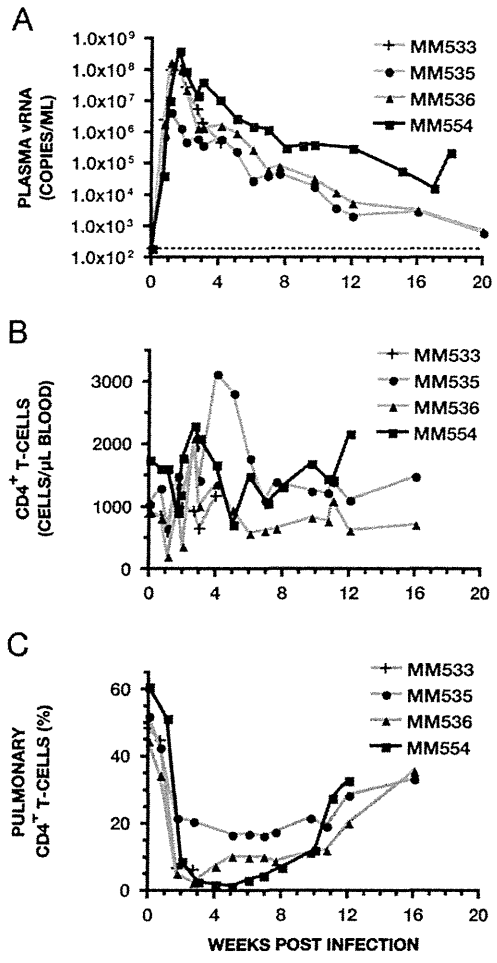

Fig. 7. Experimental infection of rhesus macaques with SHIV 97ZA012. 1×10^5 TCID50 SHIV 97ZA012 animal challenge stock was intravenously inoculated into three rhesus macaques, MM533, MM535, and MM536. Their plasma viral burdens (A), circulating $CD4^+$ T lymphocytes (B), and $CD4^+$ T cells in the alveolar space (C) were monitored periodically. Lymph node cells and whole blood collected from MM535 and MM536 at week 10.7 were transferred to MM554 (A–C).

viral burdens of all three animals declined somewhat, but remained at approximately 1×10^6 copies/ml between weeks 3 and 5. One of the animals, MM533, was found to be lethargic and subsequently died at week 4. The cause of death was not related to primate lentivirus infection. The plasma viral burdens of the remaining two animals gradually declined from week 6 onward, resulting in barely detectable levels at week 20 (650 copies/ml for MM535 and 740 copies/ml for MM536).

(Fig. 7B). Although all three animals experienced a transient decrease in cell numbers, the cell numbers promptly rebounded thereafter and basically stabilized after week 8 for MM535 and week 6 for MM536.

SIV and HIV-1 preferentially replicate at an "effector site," such as the mucosal tissues of the genital organs, lung, and gastrointestinal tract, where CCR5-positive effector memory $CD4^+$ T lymphocytes, the primary viral target cells, predominantly reside. Here, they cause substantial depletion of cells during the acute phase of infection (Brenchley et al., 2004; Okoye et al., 2007; Veazey et al., 1998; Veazey et al., 2003). Because SHIV 97ZA012 utilizes the CCR5 molecule as an entry coreceptor, it was envisaged that the virus depletes effector memory $CD4^+$ T lymphocytes as do SIV and HIV-1. We examined the fluctuation in $CD4^+$ T lymphocytes in the pulmonary space of SHIV 97ZA012-infected animals as the representative effector site because the procedure causes the least severe insult to animals, allowing us to conduct frequent monitoring. It is known that SIV239 infection results a substantial depletion of pulmonary $CD4^+$ T cells in infected rhesus macaques, along with depletion of the cells in the gastrointestinal tract (Okoye et al., 2007). In contrast to the cells in circulation, $CD4^+$ T cells in the alveolar space exhibited a substantial decline during the acute phase of SHIV 97ZA012 infection (Fig. 7C). The percentages of cells dropped from 48.5%, 52.1%, and 44.7% for MM533, MM535, and MM536, respectively, on day 0 to 6.3% for MM533 at week 2.7, 16.8% for MM535 at week 5, and 2.6% for MM536 at week 2.7. The alveolar $CD4^+$ T lymphocytes remained at low levels in the animals until week 11, then gradually increased toward pre-infection levels. Based on the results described above, it was concluded that SHIV 97ZA012 robustly replicated during the acute phase of infection, causing remarkable reduction of $CD4^+$ T cells in the alveolar space. However, the animals eventually controlled the virus replication. SHIV 97ZA012 thus appeared to be less likely to cause disease in monkeys.

Multiple reports on the evolution of primate lentivirus through animal-to-animal passage have shown that initially less-efficiently replicating and non-pathogenic viruses transform to replication-competent and highly pathogenic viruses (Joag et al., 1996; Reimann et al., 1996a; Sharma et al., 1992). We applied this strategy to SHIV 97ZA012. At week 10.7, the axillary lymph nodes were collected from animals MM535 and MM536. Cells prepared from the lymph nodes from both animals, 5×10^8 cells in total, were resuspended with 10 ml anti-coagulated whole blood collected simultaneously from these monkeys. The resuspension was intravenously transferred to another rhesus macaque, MM554. The virological and immunological parameters of the recipient animal were monitored as described above. The virus induced viremia with an initial peak of 4.2×10^8 copies/ml at week 1.6, followed by a gradual decrease until week 8, then was maintained at approximately 3–4 $\times 10^5$ copies/ml for 4 weeks (Fig. 7A). Although the plasma viral burden of MM554 declined after the initial peak, its titer was constantly higher than those inoculated with the original animal challenge stock of SHIV 97ZA012, indicating likely improvement in virus replication. Numbers of circulating $CD4^+$ T lymphocytes in MM554 did not change substantially compared with the other animals (Fig. 7B). MM554 manifested a more substantial reduction in alveolar $CD4^+$ T cells than did the other three animals (Fig. 7C). The percentage of $CD4^+$ T lymphocytes dropped from 61% at day 0 to 2.8% at week 3, and further declined to 1.4% at week 5. The cell numbers remained low until week 7 and started to recover thereafter. Based on these results, we concluded that animal-to-animal passage appears to have made SHIV 97ZA012 more fit to replicate in macaque monkeys, warranting improvement by further passage.

Discussion

In this study, we successfully generated a new SHIV strain carrying Env derived from an HIV-1 subtype C primary isolate, HIV-1 97ZA012, utilizing IHR. The presumable advantages of the method employed in the current study over conventional methods utilizing existing/newly generated restriction sites are random utilization of breakpoints within homologous sequences and selection of replication-competent recombinants through multi-round replication in the susceptible cells. These factors may have contributed to the generation of the new SHIV in the current study.

Initially, SHIVs have been generated through recombination of infectious molecular clones of SIV and HIV-1 (Shibata et al., 1991 #143; Li et al., 1992 #141; Luciw et al., 1995 #152; Reimann

et al., 1996b #153). The availability of HIV-1 infectious molecular clone(s) was thus a prerequisite for the generation of SHIV. The SHIVs generated in the abovementioned manner generally exhibited insubstantial replication profiles *in vitro* and *in vivo* (Shibata et al., 1991 #143; Li et al., 1992 #141; Sakuragi et al., 1992 #151; Luciw et al., 1995 #152; Reimann et al., 1996b #153}. Plasmid clones carrying open reading frames that were derived from PCR fragments amplified from HIV-1 provirus were subsequently employed as the source of HIV-1 genes, instead of DNA fragments excised from full-length molecular clones (Chen et al., 2000 #1; Kuwata et al., 2002 #135}. Kuwata et al. generated 30 SHIV clones representing Env protein from three independent isolates of HIV-1 from the initial exertion to generate SHIV strains representing six separate HIV-1 isolates. Of 30 clones, three were infectious to human cells, and only one productively replicated in monkey PBMCs but exhibited only modest replication *in vivo* {Kuwata et al., 2002 #135}. Hence, generation of replication-competent SHIVs by the conventional method is inefficient.

In contrast, the IHR-mediated method described in the current study generated replication-competent SHIV 97ZA012 without the requirement for an infectious molecular clone of the parental HIV-1, exploration of appropriate restriction sites, or examination of each plasmid clone for infectivity. This was performed in a considerably shorter time frame in our experience, saving several months compared with conventional methods. However, one would argue that IHR-mediated generation of SHIV does not allow for a detailed genetic analysis, such as mutagenesis of particular gene(s), because of the virus being "swarm." While this is undeniable, the vast majority of currently available replication-competent SHIVs are resultants of evolution through animal-to-animal passage and exist as quasispecies (Joag et al., 1996 #49; Reimann et al., 1996a #52; Igarashi et al., 1999 #156; Harouse et al., 2001 #154; Song et al., 2006 #158; Nishimura et al., 2010 #157}. A molecular-cloned virus representing the properties of the swarm is attainable by introduction of consensus sequences to a molecular clone, if necessary.

Co-transfection of genome fragments into C8166-CCR5 cells appears to have generated multiple recombinant viruses with distinct breakpoints and/or *env* genes. Following short-term propagation of the virus that emerged after co-transfection, viral genomic RNA from culture supernatant was subjected to sequencing without a cloning step. We were unable to determine the sequence within the overlaps between Fragments I and III or II-a/b and III (Fig. 1) because of multiple sequence peaks at each location, suggesting the existence of multiple DNA templates (data not shown). The mixture of recombinants was substantially "purified" through serial passages in RhPBMCs (Fig. 2), allowing us to determine breakpoints (Fig. 3). This observation supports the relevance of the concept employed in the current study; that is, selection of replication-competent recombinants through multi-round replication.

The selected replication-competent recombinant virus possesses breakpoints within the *env* gene, resulting in a "mosaic" *env* structure. Because primate lentiviruses encode multiple genes in different reading frames in a stratified fashion, *tat* and *rev* genes also became mosaic. The mosaic *tat*, *rev*, and *env* genes are not uncommon among circulating recombinant forms of HIV-1 (Carr et al., 2001; Koulinska et al., 2001; Ng et al., 2012; Su et al., 2000; Yamaguchi et al., 2008), although these breakpoints are less likely to be employed in rational construction of SHIVs.

SHIV 97ZA012 replicated to a titer comparable with that of SIV239 in RhPBMCs, and the observed trend was unaffected by the reduction in MOI (from 0. 1 to 0.01 in Fig. 4B), an indication of the replication competence of SHIV 97ZA012 in the cells. In addition, SHIV 97ZA012 exhibited productive replication in rhesus primary alveolar macrophages, although not as robust as that of SIV316 (Fig. 6). In our experience, not every "macrophage-tropic" virus replicates in alveolar macrophages. While SIV 251 and SIVsmE543 have been reported to be macrophage-tropic in monocyte-derived macrophages (Hirsch et al., 1997; Miller et al., 1998), they did not replicate in alveolar macrophages (Igarashi et al., unpublished). Alveolar macrophages of human or rhesus macaque express miniscule amounts of CD4 and CCR5 (Mori et al., 2000; Worgall et al., 1999). Therefore, SHIV 97ZA012 may be able to gain entry to cells expressing minimal numbers of receptors/coreceptors, as is SIV316 (Puffer et al., 2002). Whether "CD4-independence" is a property shared by many subtype-C Env or is specific to 97ZA012 or whether a "mosaic" Env protein between HIV-1 89.6 and 97ZA012 caused this notable property remains to be investigated.

This study also presents potential shortcomings of IHR to be resolved in the future. The first drawback is that only a limited variety of Env may function in the C8166-CCR5 cells utilized in the current study, resulting in generation of SHIVs reflecting this potential restriction. Prior to the current study, we inoculated nine primary isolates of HIV-1 subtype C obtained from the National Institutes of Health (NIH) AIDS Research & Reference Reagent Program into the cells and found that seven of them replicated in the cells with syncytia (data not shown). Cells susceptible to a broad range of HIV-1 primary isolates should be utilized in the future. The second shortcoming is the relatively long (2-week) "incubation phase" following co-transfection. The low frequency of recombination events and less-efficient DNA transfection may have been responsible for the elongated incubation period. Upregulation of IHR through certain means, such as overexpression of Rad51 (Vispe et al., 1998) (an enzyme that plays an important role in IHR) prior to co-transfection of viral cDNA fragments or utilization of certain cells that are shown to exhibit elevated IHR activity (e.g., breast cancer cells (Mao et al., 2009)) could augment the efficiency of recombination. To achieve higher transfection efficiency, utilization of well-established and highly transfectable cells, such as 293 T (formerly 293tsA1609neo) cells (DuBridge et al., 1987), followed by co-cultivation with cells susceptible to virus replication, such as PBMCs, should be explored.

We were able to detect syncytia formation in the culture transfected with DNA fragments only after 2 weeks. Once syncytia emerged, however, the virus replicated productively in C8166-CCR5 cells and subsequently in RhPBMCs enriched with $CD4^+$ cells and unmanipulated RhPBMCs through a passage in RhPBMCs. SHIV 97ZA012 evolved to be replication competent in RhPBMCs and infectious to RhAMs. The virus may have been replication competent in monkey cells from the beginning. Although HIV-1 97ZA012, which contributed *env* to SHIV 97ZA012, may have been predisposed to be adequate as a parental virus for generation of SHIV, we have the impression that the method we employed in this study generated a pool of recombinants and selected suitable one(s) through *in vitro* passage. As mentioned above, the recombinant virus that initially emerged was a mixture, and the final genotype(s) was selected and/or evolved through *in vitro* passage. The only traits of HIV-1 97ZA012 of which we were aware were its replication competence in human PBMCs and its preference for CCR5 as an entry co-receptor to the cells (data not shown).

SHIV 97ZA012 reproducibly replicated to high titers *in vivo* with a major reduction in pulmonary $CD4^+$ T cells during the acute phase of infection. Considering the paucity of available SHIV strains carrying subtype C Env and a CCR5 co-receptor preference in the field, the virus generated in the current study would immediately fit the interest for evaluation of anti-subtype C vaccine candidates. The virus would be especially useful when the efficacy of antiviral interventions is judged by reduction of the

initial peak viral load or prevention of virus-induced depletion of $CD4^+$ T lymphocytes in the effector sites.

Although we successfully generated an SHIV strain competent in tissue culture, the generation of a proficient virus *in vivo* remains arduous. Indeed, SHIV 97ZA012 replicated to substantially high titers during the acute phase of infection. However, the plasma viral load waned with time, as did SHIV strains generated previously. Animal-to-animal passage would augment its replication *in vivo*, as we attempted in this study.

This study has demonstrated the versatility of IHR-mediated generation of SHIV. The method enables utilization of a PCR fragment amplified from uncloned virus as a source for SHIV. This method can be further extended to generate SHIV strains with sequences amplified from clinical samples, such as patient plasma, to strengthen the panel of challenging viruses for evaluation of an anti-HIV vaccine.

Conclusions

By employing IHR, a replication-competent SHIV carrying Env derived from a CCR5-tropic, subtype C HIV-1 97ZA012 strain was generated.

Materials and methods

Cells

C8166-CCR5 cells from a human T-lymphotropic virus type-1-transformed human T-lymphoid cell line that was transduced to express human CCR5 and established as described previously (Soda et al., 1999) were generously provided by Dr. Hiroo Hoshino, Gunma University, Japan. The cells were cultured in Roswell Park Memorial Institute 1640 medium (Life Technologies Corporation, Grand Island, NY, USA) supplemented with 10% fetal bovine serum, 4 mM L-glutamine, and 2 mM sodium pyruvate (*R*-10). RhPBMCs were prepared and cultured as described previously (Imamichi et al., 2002), with minor modification; 160 units/ml recombinant interleukin-2 (Wako Pure Chemicals, Osaka, Japan) was added to the medium to maintain lymphocytes. RhAMs were collected through a bronchoalveolar lavage technique and cultured as described previously (Imamichi et al., 2002).

Viruses

Virus stocks of SIV239 (Kestler et al., 1988), SIV316 (Desrosiers et al., 1991), SHIV DH12R CL7 (Sadjadpour et al., 2004), and SHIV λ3-3 (Igarashi et al., 2007) were propagated in RhPBMCs following inoculation with transfection supernatant of the proviral plasmid of each virus. Dr. Ronald C. Desrosiers at Harvard University kindly provided the plasmid of SIV239. Dr. Malcolm A. Martin at the National Institute of Allergy and Infectious Diseases (NIAID), NIH, generously contributed the plasmid of SIV316 with permission from Dr. Desrosiers and the plasmids of SHIV DH12R CL-7 and SHIV λ3-3. Infectious titers ($TCID_{50}$) of the virus stocks were determined by titration as described previously (Shibata et al., 1997), with a minor modification; the indicator cells employed for titration were RhPBMCs in this study. The HIV-1 97ZA012 isolate was obtained from The UNAIDS Network for HIV Isolation and Characterization through the AIDS Research and Reference Reagent Program, Division of AIDS, NIAID, NIH, and was propagated briefly in human PBMCs after acquisition.

Preparation of cDNA from HIV-1 97ZA012 genomic RNA

Culture supernatant was harvested from human PBMCs infected with HIV-1 97ZA012 on day 8 post-inoculation. Virion-associated RNA was extracted with the QIAamp Viral RNA mini kit (QIAGEN, Hilden, Germany), following the manufacturer's instructions. The extracted RNA was subsequently subjected to synthesis of cDNA with Super Script III (Life Technologies Corporation) following the manufacturer's instructions. For the reaction, the following primer was utilized: OFM19-R (5′-aggcaagctttattgaggctta-3′ at 9604-9625 in HIV-1 HXB2).

Generation of recombinant virus through IHR

Two segments of the SHIV genome (Fragments I and II; Fig. 1) were amplified by PCR with pSHIV KS661, an infectious molecular clone of SHIV C2/1 (Shinohara et al., 1999), as a template. Positions of PCR primers were numbered relative to the SIV239 or HIV-1 HXB2 genome sequence (GenBank accession nos. M33262 and K03455, respectively). For Fragment I, the following primer pair was employed: SIVU3Not-F forward primer (5′-atgcggccgctggaaggg-gatttattacagtgcaag-3′, at 1–25 in SIV239) and SHenv2R rear primer (5′-cacagagtggggttaattttacac-3′, at 6580–6603 in HIV-1 HXB2). Two sets of Fragment II (II-a and II-b) were amplified by PCR. For Fragment II-a, the following primer pair was used: SHenv5.5F forward primer (5′-tcataatgatagtaggaggc-3′, at 8278–8297 in HIV-1 HXB2) and SIVU5Eco-R rear primer (5′-tgcagaattctgctagggat-tttcctgcttcggtt-3′, at 10255–10279 in SIV239). For Fragment II-b, the following primer pair was utilized: SHenv6F forward primer (5′-gcggagcctgtgcctcttcagc-3′, at 8504–8525 in HIV-1 HXB2) and SIVU5Eco-R rear primer. A segment of the HIV-1 97ZA012 genome containing *env* and flanking genes (Fragment III) was amplified through PCR with cDNA of viral genomic RNA as a template. For amplification of Fragment III, the following primer pair was applied: HIVvpr-F forward primer (5′-agatggaacaagccccagaaga-3′ at 5557–5578 in HIV-1 HXB2) and OFM19-R rear primer.

All PCR reactions were conducted with the Expand Long Range dNTPack (Roche Diagnostic Corporation, Basel, Switzerland) under the following conditions: initial denaturation at 94 °C for 2 min, followed by 10 cycles of amplification consisting of denaturation at 94 °C for 15 s, annealing at 55 °C for 30 s, and extension at 68 °C for 8 min. The reaction was continued with 25 cycles of amplification consisting of denaturation at 94 °C for 15 s, annealing at 55 °C for 30 s, and extension at 68 °C for 8 min (plus 20 s at every cycle), followed by a final extension at 68 °C for 7 min.

Mixtures of Fragments I, II-a, and III (Transfection #1) or I, II-b, and III (Transfection #2), 0.2 μg of each fragment, were co-transfected into C8166-CCR5 cells through diethylaminoethyl-dextran-mediated DNA uptake followed by osmotic shock (Takai and Ohmori, 1990). After co-transfection, the cell cultures were maintained in 24-well plates at 37 °C and monitored by daily microscopic observation. On day 14 for Transfection #1 and day 15 for Transfection #2, a small portion of each culture was taken and independently co-cultured with uninfected C8166-CCR5 cells for an additional 3 days.

In vitro passage of recombinant virus

RhPBMCs were prepared as described above. The $CD8^+$ cell fraction was removed from the cell preparation using phycoerythrin (PE)-conjugated anti-CD8 antibody (clone SK1; BD BioSciences, San Jose, CA, USA) and anti-PE-conjugated magnetic microbeads (Miltenyi Biotec GmbH, Bergisch Gladbach, Germany), following the manufacturers' instructions.

Culture supernatant from C8166-CCR5 cells co-cultured with Transfection #1 or Transfection #2 on days 17 and 18 post-transfection, respectively, was mixed and filtered through a 0.45-μm membrane. The supernatant, 100 μl in total, was subsequently inoculated into 2×10^6 $CD4^+$ cell-enriched RhPBMCs (Passage #1). Freshly prepared $CD4^+$ cell-enriched RhPBMCs, 2×10^6 cells in total, were added to Passage #1 on day 3 post-inoculation. Virus replication was assessed by virion-associated RT activity in the culture supernatant, as described below. Cryopreserved supernatant on day 5 (50 μl) from Passage #1 was thawed and inoculated into 2×10^6 $CD4^+$ cell-enriched RhPBMCs (Passage #2). On day 3, freshly prepared $CD4^+$ cell-enriched RhPBMCs, 2×10^6 cells in total, were added to Passage #2. The RT activity of the supernatant was monitored daily, and a small portion of Passage #2 on day 8, when the RT activity rose substantially, was subsequently co-cultured with 2×10^6 freshly isolated RhPBMCs without enrichment of $CD4^+$ cells (Passage #3). On day 3, 2×10^6 freshly prepared $CD4^+$ cell-enriched RhPBMCs were added to Passage #3. Cryopreserved supernatant from Passage #3 on day 7 (50 μl) was thawed and inoculated into 2×10^6 freshly prepared RhPBMCs without manipulation (Passage #4). On day 3, 2×10^6 freshly prepared RhPBMCs without manipulation were added to Passage #4. Cryopreserved supernatant from Passage #4 on day 5 (50 μl) was thawed and inoculated into 2×10^6 freshly prepared RhPBMCs without manipulation (Passage #5). Fresh RhPBMCs without manipulation were added to Passage #5 on day 3.

Reverse transcriptase assay

Virion-associated RT activity in the culture supernatant was evaluated as described previously (Willey et al., 1988), with a minor modification; α-^{32}P TTP was purchased from PerkinElmer Inc. (Waltham, MA, USA) in this study.

Genomic analysis of the recombinant virus

Virion-associated viral genomic RNA was extracted from culture supernatant collected on day 5 of Passage #5 and reverse transcribed, as described above. For sequencing, the bulk cDNA was directly subjected to the Sanger dideoxy method with a BigDye Terminator Cycle Sequencing Kit (Life Technologies Corporation) and analyzed with an ABI PRISM 3130 Genetic Analyzer (Life Technologies Corporation).

Breakpoints of the recombinant virus were determined through comparison of sequences of the recombinant virus with those of SHIV KS661 (identical to SHIV C2/1, GenBank accession no. AF217181) and p97ZA012 (GenBank accession no. AF286227). The sequences were aligned using Clustal X software (Thompson et al., 1997) and analyzed using SimPlot software (Lole et al., 1999), with a window size of 250 bp and a step size of 20 bp.

A portion of the nt sequence of SHIV 97ZA012, at nt 6429–8325 (in HIV-1 HXB2) and derived from HIV-1 97ZA012, was subjected to phylogenetic analysis with the corresponding sequence of the following reference virus isolates: 93IN905 (GenBank accession no. AY669742), 98CN009 (AF286230), 98CN006 (AF286229), 98TZ017 (AF286235), 97ZA009 (AY118166), and 97ZA012 (AF286227) for subtype *C* references, and DH12.3 (AF069140), JR-FL (U63632), ADA.AD8 (AF004394), SF162 (EU123924), HXB2 (K03455), and SHIV KS661 for subtype *B* references. Phylogenetic analysis by neighbor-joining method (Saitou and Nei, 1987) was conducted using Clustal X software. The analyzed result was plotted by Mega 5 software (Tamura et al., 2011).

Replication kinetics of SHIV 97ZA012

Virus stocks subjected to comparison were normalized to the infectious titer (MOI=0.01 or 0.1 $TCID_{50}$/cell). For infection of M8166-CCR5 cells, HIV-1 97ZA012, SHIV KS661, and SHIV 97ZA012 were titrated using TZM-bl cells, which were granted from the NIH AIDS Research & Reference Reagent Program. For infection of RhPBMCs, SIV239 and SHIV 97ZA012 were titrated in RhPBMCs. The virus stocks were inoculated to C8166-CCR5 cells or RhPBMCs by spinoculation (O'Doherty et al., 2000) at $1200 \times g$ for 60 min.

After inoculation, culture supernatant was replaced daily with freshly prepared medium and stored at −20 °C until analysis of its RT activity. The AUC of the replication kinetics, an estimate of the total production of progeny virus during the observation period, was calculated for each virus using the Prism 4 Software (GraphPad Software, Inc., La Jolla, CA, USA).

Co-receptor usage assay

The co-receptor preference of SHIV 97ZA012 on RhPBMCs was analyzed as described previously (Matsuda et al., 2010), with the modifications described below. Infectious titers of SHIV 97ZA012, SIV239, and SHIV DH12R CL7 were normalized by the infectious titer (MOI=0.03 $TCID_{50}$/cell) in this study. In the presence of 5 μM of the small-molecule co-receptor inhibitors AMD3100 (De Clercq et al., 1994) (Sigma-Aldrich, St. Louis, MO, USA), AD101 (Trkola et al., 2002), or both, the viruses were spinoculated ($1200 \times g$ for 60 min) into RhPBMCs, and virus replication was monitored for 7 days. During the experiment, culture supernatant was replaced on days 1, 3, and 5 with freshly prepared culture medium containing the same concentration of corresponding inhibitor(s). Culture supernatant was collected on days 1, 3, 5, and 7 and stored at −20 °C until assessment of RT activity. Dr. Julie Strizki, Schering-Plough Research Institute, Kenilworth, NJ, generously provided the AD101.

Replication of SHIV 97ZA012 in RhAMs

RhAMs were collected and cultured as described above. SHIV 97ZA012, SIV239, SIV316, and SHIV λ3-3 were normalized by RT activity (MOI=17 cpm equivalent/cell) and spinoculated ($1200 \times g$ for 60 min) to 5×10^5 cells in a 24-well plate. Culture supernatant was replaced every other day with freshly prepared medium and stored at −20 °C until assessment of its RT activity.

Experimental infection of rhesus monkeys with SHIV 97ZA012

Rhesus macaques of Indian origin, approximately 4 kg in body weight, were used for experimental infection with SHIV 97ZA012. Phlebotomy, bronchoalveolar lavage, lymph node biopsy, and virus inoculation were conducted under anesthesia by intramuscular injection of a mixture of ketamine chloride (Ketalar; Daiichi Sankyo, Tokyo, Japan) at 5–10 mg/kg and xylazine chloride (Celactal; Bayer Healthcare, Leverkusen, Germany) at 1.5–2.0 mg/kg. Animals 533, 535, and 536 were intravenously inoculated with 1×10^5 $TCID_{50}$ SHIV 97ZA012. Animal 554 intravenously received a mixture of anticoagulated whole blood (10 ml) and lymph node cells (5×10^8 cells) collected from animals 535 and 536 at 10.7 weeks post-inoculation. All animal experiments were conducted in a biosafety level 3 animal facility in compliance with institutional regulations approved by the Committee for Experimental Use of Nonhuman Primates of the Institute for Virus Research, Kyoto University, Kyoto, Japan.

Acknowledgments

The authors thank Drs. Julie Strizki and Paul Zavodny for providing AD101, the NIH AIDS Research & Reference Reagent Program for providing primary isolates of HIV-1 and TZM-bl cells, Dr. A. Nomoto for continuous support, and members of the Igarashi laboratory for assistance with animal procedures and analyses. This work was supported by a Research on HIV/AIDS grant [awarded to T.M. and T.I., independently] from The Ministry of Health, Labor and Welfare of Japan, and by a Grant-in-Aid for Scientific Research (B) [awarded to T.M. and T.I., independently] from the Japan Society for the Promotion of Science.

References

Brenchley, J.M., Schacker, T.W., Ruff, L.E., Price, D.A., Taylor, J.H., Beilman, G.J., Nguyen, P.L., Khoruts, A., Larson, M., Haase, A.T., Douek, D.C., 2004. CD4+ T cell depletion during all stages of HIV disease occurs predominantly in the gastrointestinal tract. J. Exp. Med. 200, 749–759.

Broder, C.C., Jones-Trower, A., 1999. Coreceptor Use by Primate Lentiviruses, Human Retroviruses and AIDS. Theoretical Biology and Biophysics Group. Los Alamos National Laboratory, Los Alamos, NM.

Carr, J.K., Avila, M., Gomez Carrillo, M., Salomon, H., Hierholzer, J., Watanaveeradej, V., Pando, M.A., Negrete, M., Russell, K.L., Sanchez, J., Birx, D.L., Andrade, R., Vinoles, J., McCutchan, F.E., 2001. Diverse BF recombinants have spread widely since the introduction of HIV-1 into South America. Aids 15, F41–47.

Chen, Z., Huang, Y., Zhao, X., Skulsky, E., Lin, D., Ip, J., Gettie, A., Ho, D.D., 2000. Enhanced infectivity of an R5-tropic simian/human immunodeficiency virus carrying human immunodeficiency virus type 1 subtype C envelope after serial passages in pig-tailed macaques (Macaca nemestrina). J. Virol. 74, 6501–6510.

Cheng-Mayer, C., Quiroga, M., Tung, J.W., Dina, D., Levy, J.A., 1990. Viral determinants of human immunodeficiency virus type 1 T-cell or macrophage tropism, cytopathogenicity, and CD4 antigen modulation. J. Virol. 64, 4390–4398.

Clavel, F., Hoggan, M.D., Willey, R.L., Strebel, K., Martin, M.A., Repaske, R., 1989. Genetic recombination of human immunodeficiency virus. J. Virol. 63, 1455–1459.

De Clercq, E., Yamamoto, N., Pauwels, R., Balzarini, J., Witvrouw, M., De Vreese, K., Debyser, Z., Rosenwirth, B., Peichl, P., Datema, R., et al., 1994. Highly potent and selective inhibition of human immunodeficiency virus by the bicyclam derivative JM3100. Antimicrob. Agents Chemother. 38, 668–674.

Desrosiers, R.C., Hansen-Moosa, A., Mori, K., Bouvier, D.P., King, N.W., Daniel, M.D., Ringler, D.J., 1991. Macrophage-tropic variants of SIV are associated with specific AIDS-related lesions but are not essential for the development of AIDS. Am. J. Pathol. 139, 29–35.

DuBridge, R.B., Tang, P., Hsia, H.C., Leong, P.M., Miller, J.H., Calos, M.P., 1987. Analysis of mutation in human cells by using an Epstein-Barr virus shuttle system. Mol. Cell. Biol. 7, 379–387.

Gorry, P.R., Bristol, G., Zack, J.A., Ritola, K., Swanstrom, R., Birch, C.J., Bell, J.E., Bannert, N., Crawford, K., Wang, H., Schols, D., De Clercq, E., Kunstman, K., Wolinsky, S.M., Gabuzda, D., 2001. Macrophage tropism of human immunodeficiency virus type 1 isolates from brain and lymphoid tissues predicts neurotropism independent of coreceptor specificity. J. Virol. 75, 10073–10089.

Guimaraes, M.L., Eyer-Silva, W.A., Couto-Fernandez, J.C., Morgado, M.G., 2008. Identification of two new CRF_BF in Rio de Janeiro State, Brazil. Aids 22, 433–435.

Harouse, J.M., Gettie, A., Eshetu, T., Tan, R.C., Bohm, R., Blanchard, J., Baskin, G., ChengMayer, C., 2001. Mucosal transmission and induction of simian AIDS by CCR5-specific simian/human immunodeficiency virus SHIV(SF162P3). J. Virol. 75, 1990–1995.

Hemelaar, J., Gouws, E., Ghys, P.D., Osmanov, S., 2011. Global trends in molecular epidemiology of HIV-1 during 2000-2007. Aids 25, 679–689.

Hertogs, K., de Bethune, M.P., Miller, V., Ivens, T., Schel, P., Van Cauwenberge, A., Van Den Eynde, C., Van Gerwen, V., Azijn, H., Van Houtte, M., Peeters, F., Staszewski, S., Conant, M., Bloor, S., Kemp, S., Larder, B., Pauwels, R., 1998. A rapid method for simultaneous detection of phenotypic resistance to inhibitors of protease and reverse transcriptase in recombinant human immunodeficiency virus type 1 isolates from patients treated with antiretroviral drugs. Antimicrob. Agents Chemother. 42, 269–276.

Hirsch, V., Adger-Johnson, D., Campbell, B., Goldstein, S., Brown, C., Elkins, W.R., Montefiori, D.C., 1997. A molecularly cloned, pathogenic, neutralization-resistant simian immunodeficiency virus, SIVsmE543-3. J. Virol. 71, 1608–1620.

Igarashi, T., Endo, Y., Englund, G., Sadjadpour, R., Matano, T., Buckler, C., Buckler-White, A., Plishka, R., Theodore, T., Shibata, R., Martin, M., 1999. Emergence of a highly pathogenic simian/human immunodeficiency virus in a rhesus macaque treated with anti-CD8 mAb during a primary infection with a nonpathogenic virus. Proc. Natl. Acad. Sci. USA 96, 14049–14054.

Igarashi, T., Donau, O.K., Imamichi, H., Nishimura, Y., Theodore, T.S., Iyengar, R., Erb, C., Buckler-White, A., Buckler, C.E., Martin, M.A., 2007. Although macrophage-tropic simian/human immunodeficiency viruses can exhibit a range of pathogenic phenotypes, a majority of isolates induce no clinical disease in immunocompetent macaques. J. Virol. 81, 10669–10679.

Igarashi, T., Donau, O.K., Matsuyama, M., Unpublished Results.

Imamichi, H., Igarashi, T., Imamichi, T., Donau, O.K., Endo, Y., Nishimura, Y., Willey, R.L., Suffredini, A.F., Lane, H.C., Martin, M.A., 2002. Amino acid deletions are introduced into the V2 region of gp120 during independent pathogenic simian immunodeficiency virus/HIV chimeric virus (SHIV) infections of rhesus monkeys generating variants that are macrophage tropic. Proc. Natl. Acad. Sci. USA 99, 13813–13818.

Inoue, M., Hoxie, J.A., Reddy, M.V., Srinivasan, A., Reddy, E.P., 1991. Mechanisms associated with the generation of biologically active human immunodeficiency virus type 1 particles from defective proviruses. Proc. Natl. Acad. Sci. USA 88, 2278–2282.

Joag, S.V., Li, Z., Foresman, L., Stephens, E.B., Zhao, L.J., Adany, I., Pinson, D.M., McClure, H.M., Narayan, O., 1996. Chimeric simian/human immunodeficiency virus that causes progressive loss of CD4+ T cells and AIDS in pig-tailed macaques. J. Virol. 70, 3189–3197.

John-Stewart, G.C., Nduati, R.W., Rousseau, C.M., Mbori-Ngacha, D.A., Richardson, B.A., Rainwater, S., Panteleeff, D.D., Overbaugh, J., 2005. Subtype C is associated with increased vaginal shedding of HIV-1. J. Infect. Dis. 192, 492–496.

Kalyanaraman, S., Jannoun-Nasr, R., York, D., Luciw, P.A., Robinson, R., Srinivasan, A., 1988. Homologous recombination between human immunodeficiency viral DNAs in cultured human cells: analysis of the factors influencing recombination. Biochem. Biophys. Res. Commun. 157, 1051–1060.

Kamada, K., Igarashi, T., Martin, M.A., Khamsri, B., Hatcho, K., Yamashita, T., Fujita, M., Uchiyama, T., Adachi, A., 2006. Generation of HIV-1 derivatives that productively infect macaque monkey lymphoid cells. Proc. Natl. Acad. Sci. USA 103, 16959–16964.

Kellam, P., Larder, B.A., 1994. Recombinant virus assay: a rapid, phenotypic assay for assessment of drug susceptibility of human immunodeficiency virus type 1 isolates. Antimicrob. Agents Chemother. 38, 23–30.

Kestler 3rd, H.W., Li, Y., Naidu, Y.M., Butler, C.V., Ochs, M.F., Jaenel, G., King, N.W., Daniel, M.D., Desrosiers, R.C., 1988. Comparison of simian immunodeficiency virus isolates. Nature 331, 619–622.

Koulinska, I.N., Ndung'u, T., Mwakagile, D., Msamanga, G., Kagoma, C., Fawzi, W., Essex, M., Renjifo, B., 2001. A new human immunodeficiency virus type 1 circulating recombinant form from Tanzania. AIDS Res. Hum. Retroviruses 17, 423–431.

Kuwata, T., Takemura, T., Takehisa, J., Miura, T., Hayami, M., 2002. Infection of macaques with chimeric simian and human immunodeficiency viruses containing Env from subtype F. Arch. Virol. 147, 1121–1132.

Li, J., Lord, C.I., Haseltine, W., Letvin, N.L., Sodroski, J., 1992. Infection of cynomolgus monkeys with a chimeric HIV-1/SIVmac virus that expresses the HIV-1 envelope glycoproteins. J. Acquired Immune Defic. Syndromes 5, 639–646.

Lole, K.S., Bollinger, R.C., Paranjape, R.S., Gadkari, D., Kulkarni, S.S., Novak, N.G., Ingersoll, R., Sheppard, H.W., Ray, S.C., 1999. Full-length human immunodeficiency virus type 1 genomes from subtype C-infected seroconverters in India, with evidence of intersubtype recombination. J. Virol. 73, 152–160.

Luciw, P.A., Pratt-Lowe, E., Shaw, K.E., Levy, J.A., Cheng-Mayer, C., 1995. Persistent infection of rhesus macaques with T-cell-line-tropic and macrophage-tropic clones of simian/human immunodeficiency viruses (SHIV). Proc. Natl. Acad. Sci. USA 92, 7490–7494.

Mao, Z., Jiang, Y., Liu, X., Seluanov, A., Gorbunova, V., 2009. DNA repair by homologous recombination, but not by nonhomologous end joining, is elevated in breast cancer cells. Neoplasia 11, 683–691.

Matsuda, K., Inaba, K., Fukazawa, Y., Matsuyama, M., Ibuki, K., Horiike, M., Saito, N., Hayami, M., Igarashi, T., Miura, T., 2010. *In vivo* analysis of a new R5 tropic SHIV generated from the highly pathogenic SHIV-KS661, a derivative of SHIV-89.6. Virology 399, 134–143.

Miller, C.J., Marthas, M., Greenier, J., Lu, D., Dailey, P.J., Lu, Y., 1998. *In vivo* replication capacity rather than *in vitro* macrophage tropism predicts efficiency of vaginal transmission of simian immunodeficiency virus or simian/human immunodeficiency virus in rhesus macaques. J. Virol. 72, 3248–3258.

Moore, P.L., Gray, E.S., Choge, I.A., Ranchobe, N., Mlisana, K., Abdool Karim, S.S., Williamson, C., Morris, L., 2008. The c3-v4 region is a major target of autologous neutralizing antibodies in human immunodeficiency virus type 1 subtype C infection. J. Virol. 82, 1860–1869.

Mori, K., Ringler, D.J., Desrosiers, R.C., 1993. Restricted replication of simian immunodeficiency virus strain 239 in macrophages is determined by env but is not due to restricted entry. J. Virol. 67, 2807–2814.

Mori, K., Rosenzweig, M., Desrosiers, R.C., 2000. Mechanisms for adaptation of simian immunodeficiency virus to replication in alveolar macrophages. J. Virol. 74, 10852–10859.

Ng, O.T., Eyzaguirre, L.M., Carr, J.K., Chew, K.K., Lin, L., Chua, A., Leo, Y.S., Redd, A.D., Quinn, T.C., Laeyendecker, O., 2012. Identification of new CRF51_01B in Singapore using full genome analysis of three HIV type 1 isolates. AIDS Res. Hum. Retroviruses 28, 527–530.

Nishimura, Y., Shingai, M., Willey, R., Sadjadpour, R., Lee, W.R., Brown, C.R., Brenchley, J.M., Buckler-White, A., Petros, R., Eckhaus, M., Hoffman, V., Igarashi, T., Martin, M.A., 2010. Generation of the pathogenic R5-tropic simian/human immunodeficiency virus SHIVAD8 by serial passaging in rhesus macaques. J. Virol. 84, 4769–4781.

O'Doherty, U., Swiggard, W.J., Malim, M.H., 2000. Human immunodeficiency virus type 1 spinoculation enhances infection through virus binding. J. Virol. 74, 10074–10080.

Okoye, A., Meier-Schellersheim, M., Brenchley, J.M., Hagen, S.I., Walker, J.M., Rohankhedkar, M., Lum, R., Edgar, J.B., Planer, S.L., Legasse, A., Sylwester, A.W., Piatak Jr., M., Lifson, J.D., Maino, V.C., Sodora, D.L., Douek, D.C., Axthelm, M.K., Grossman, Z., Picker, L.J., 2007. Progressive CD4+ central memory T cell decline results in CD4+ effector memory insufficiency and overt disease in chronic SIV infection. The Journal of experimental medicine 204, 2171–2185.

Perez, L., Thomson, M.M., Bleda, M.J., Aragones, C., Gonzalez, Z., Perez, J., Sierra, M., Casado, G., Delgado, E., Najera, R., 2006. HIV Type 1 molecular epidemiology in cuba: high genetic diversity, frequent mosaicism, and recent expansion of BG intersubtype recombinant forms. AIDS Res. Hum. Retroviruses 22, 724–733.

Piyasirisilp, S., McCutchan, F.E., Carr, J.K., Sanders-Buell, E., Liu, W., Chen, J., Wagner, R., Wolf, H., Shao, Y., Lai, S., Beyrer, C., Yu, X.F., 2000. A recent outbreak of human immunodeficiency virus type 1 infection in southern China was initiated by two highly homogeneous, geographically separated strains, circulating recombinant form AE and a novel BC recombinant. J. Virol. 74, 11286–11295.

Puffer, B.A., Pohlmann, S., Edinger, A.L., Carlin, D., Sanchez, M.D., Reitter, J., Watry, D.D., Fox, H.S., Desrosiers, R.C., Doms, R.W., 2002. CD4 independence of simian immunodeficiency virus Envs is associated with macrophage tropism, neutralization sensitivity, and attenuated pathogenicity. J. Virol. 76, 2595–2605.

Reimann, K.A., Li, J.T., Veazey, R., Halloran, M., Park, I.W., Karlsson, G.B., Sodroski, J., Letvin, N.L., 1996a. A chimeric simian/human immunodeficiency virus expressing a primary patient human immunodeficiency virus type 1 isolate env causes an AIDS-like disease after *in vivo* passage in rhesus monkeys. J. Virol. 70, 6922–6928.

Reimann, K.A., Li, J.T., Voss, G., Lekutis, C., TennerRacz, K., Racz, P., Lin, W., Montefiori, D.C., LeeParritz, D.E., Lu, Y., Collman, R.G., Sodroski, J., Letvin, N.L., 1996b. An env gene derived from a primary human immunodeficiency virus type 1 isolate confers high in vivo replicative capacity to a chimeric simian/human immunodeficiency virus in rhesus monkeys. J. Virol. 70, 3198–3206.

Sadjadpour, R., Theodore, T.S., Igarashi, T., Donau, O.K., Plishka, R.J., Buckler-White, A., Martin, M.A., 2004. Induction of disease by a molecularly cloned highly pathogenic simian immunodeficiency virus/human immunodeficiency virus chimera is multigenic. J. Virol. 78, 5513–5519.

Saitou, N., Nei, M., 1987. The neighbor-joining method: a new method for reconstructing phylogenetic trees. Mol. Biol. Evol. 4, 406–425.

Sakuragi, S., Shibata, R., Mukai, R., Komatsu, T., Fukasawa, M., Sakai, H., Sakuragi, J., Kawamura, M., Ibuki, K., Hayami, M., 1992. Infection of macaque monkeys with a chimeric human and simian immunodeficiency virus. J. Gen. Virol. 73 (Pt 11), 2983–2987.

Sharma, D.P., Zink, M.C., Anderson, M., Adams, R., Clements, J.E., Joag, S.V., Narayan, O., 1992. Derivation of neurotropic simian immunodeficiency virus from exclusively lymphocytetropic parental virus: pathogenesis of infection in macaques. J. Virol. 66, 3550–3556.

Shibata, R., Kawamura, M., Sakai, H., Hayami, M., Ishimoto, A., Adachi, A., 1991. Generation of a chimeric human and simian immunodeficiency virus infectious to monkey peripheral blood mononuclear cells. J. Virol. 65, 3514–3520.

Shibata, R., Maldarelli, F., Siemon, C., Matano, T., Parta, M., Miller, G., Fredrickson, T., Martin, M.A., 1997. Infection and pathogenicity of chimeric simian-human immunodeficiency viruses in macaques: determinants of high virus loads and CD4 cell killing. J. Infect. Dis. 176, 362–373.

Shinohara, K., Sakai, K., Ando, S., Ami, Y., Yoshino, N., Takahashi, E., Someya, K., Suzaki, Y., Nakasone, T., Sasaki, Y., Kaizu, M., Lu, Y., Honda, M., 1999. A highly pathogenic simian/human immunodeficiency virus with genetic changes in cynomolgus monkey. J. Gen. Virol. 80 (Pt 5), 1231–1240.

Soda, Y., Shimizu, N., Jinno, A., Liu, H.Y., Kanbe, K., Kitamura, T., Hoshino, H., 1999. Establishment of a new system for determination of coreceptor usages of HIV based on the human glioma NP-2 cell line. Biochem. Biophys. Res. Commun. 258, 313–321.

Song, R.J., Chenine, A.L., Rasmussen, R.A., Ruprecht, C.R., Mirshahidi, S., Grisson, R.D., Xu, W., Whitney, J.B., Goins, L.M., Ong, H., Li, P.L., ShaiKobiler, E., Wang, T., McCann, C.M., Zhang, H., Wood, C., Kankasa, C., Secor, W.E., McClure, H.M., Strobert, E., Else, J.G., Ruprecht, R.M., 2006. Molecularly cloned SHIV-1157ipd3N4: a highly replication-competent, mucosally transmissible R5 simian-human immunodeficiency virus encoding HIV clade C Env. J. Virol. 80, 8729–8739.

Srinivasan, A., York, D., Jannoun-Nasr, R., Kalyanaraman, S., Swan, D., Benson, J., Bohan, C., Luciw, P.A., Schnoll, S., Robinson, R.A., et al., 1989. Generation of hybrid human immunodeficiency virus by homologous recombination. Proc. Natl. Acad. Sci. USA 86, 6388–6392.

Su, L., Graf, M., Zhang, Y., von Briesen, H., Xing, H., Kostler, J., Melzl, H., Wolf, H., Shao, Y., Wagner, R., 2000. Characterization of a virtually full-length human immunodeficiency virus type 1 genome of a prevalent intersubtype (C/B') recombinant strain in China. J. Virol. 74, 11367–11376.

Takai, T., Ohmori, H., 1990. DNA transfection of mouse lymphoid cells by the combination of DEAE-dextran-mediated DNA uptake and osmotic shock procedure. Biochim. Biophys. Acta 1048, 105–109.

Tamura, K., Peterson, D., Peterson, N., Stecher, G., Nei, M., Kumar, S., 2011. MEGA5: molecular evolutionary genetics analysis using maximum likelihood, evolutionary distance, and maximum parsimony methods. Mol. Biol. Evol. 28, 2731–2739.

Thompson, J.D., Gibson, T.J., Plewniak, F., Jeanmougin, F., Higgins, D.G., 1997. The CLUSTAL_X windows interface: flexible strategies for multiple sequence alignment aided by quality analysis tools. Nucl. Acids Res. 25, 4876–4882.

Trkola, A., Kuhmann, S.E., Strizki, J.M., Maxwell, E., Ketas, T., Morgan, T., Pugach, P., Xu, S., Wojcik, L., Tagat, J., Palani, A., Shapiro, S., Clader, J.W., McCombie, S., Reyes, G.R., Baroudy, B.M., Moore, J.P., 2002. HIV-1 escape from a small molecule, CCR5-specific entry inhibitor does not involve CXCR4 use. Proc. Natl Acad. Sci. USA 99, 395–400.

UNAIDS, 2010. Report on the Global Aids Epidemic.

Veazey, R.S., DeMaria, M., Chalifoux, L.V., Shvetz, D.E., Pauley, D.R., Knight, H.L., Rosenzweig, M., Johnson, R.P., Desrosiers, R.C., Lackner, A.A., 1998. Gastrointestinal tract as a major site of CD4+ T cell depletion and viral replication in SIV infection. Science 280, 427–431.

Veazey, R.S., Marx, P.A., Lackner, A.A., 2003. Vaginal CD4+ T cells express high levels of CCR5 and are rapidly depleted in simian immunodeficiency virus infection. J. Infect. Dis. 187, 769–776.

Vispe, S., Cazaux, C., Lesca, C., Defais, M., 1998. Overexpression of Rad51 protein stimulates homologous recombination and increases resistance of mammalian cells to ionizing radiation. Nucl. Acids Res. 26, 2859–2864.

Walter, B.L., Armitage, A.E., Graham, S.C., de Oliveira, T., Skinhoj, P., Jones, E.Y., Stuart, D.I., McMichael, A.J., Chesebro, B., Iversen, A.K., 2009. Functional characteristics of HIV-1 subtype C compatible with increased heterosexual transmissibility. Aids 23, 1047–1057.

Willey, R.L., Smith, D.H., Lasky, L.A., Theodore, T.S., Earl, P.L., Moss, B., Capon, D.J., Martin, M.A., 1988. *In vitro* mutagenesis identifies a region within the envelope gene of the human immunodeficiency virus that is critical for infectivity. J. Virol. 62, 139–147.

Worgall, S., Connor, R., Kaner, R.J., Fenamore, E., Sheridan, K., Singh, R., Crystal, R.G., 1999. Expression and use of human immunodeficiency virus type 1 coreceptors by human alveolar macrophages. J. Virol. 73, 5865–5874.

Yamaguchi, J., Badreddine, S., Swanson, P., Bodelle, P., Devare, S.G., Brennan, C.A., 2008. Identification of new CRF43_02G and CRF25_cpx in Saudi Arabia based on full genome sequence analysis of six HIV type 1 isolates. AIDS Res. Hum. Retroviruses 24, 1327–1335.

Zhang, Y., Lou, B., Lal, R.B., Gettie, A., Marx, P.A., Moore, J.P., 2000. Use of inhibitors to evaluate coreceptor usage by simian and simian/human immunodeficiency viruses and human immunodeficiency virus type 2 in primary cells. J. Virol. 74, 6893–6910.

OPEN ACCESS Freely available online

PLOS ONE

A Novel Protective MHC-I Haplotype Not Associated with Dominant Gag-Specific CD8$^+$ T-Cell Responses in SIVmac239 Infection of Burmese Rhesus Macaques

Naofumi Takahashi[1,2], Takushi Nomura[1,2], Yusuke Takahara[1,2], Hiroyuki Yamamoto[1], Teiichiro Shiino[1], Akiko Takeda[1], Makoto Inoue[3], Akihiro Iida[3], Hiroto Hara[3], Tsugumine Shu[3], Mamoru Hasegawa[3], Hiromi Sakawaki[4], Tomoyuki Miura[4], Tatsuhiko Igarashi[4], Yoshio Koyanagi[4], Taeko K. Naruse[5], Akinori Kimura[5], Tetsuro Matano[1,2]*

1 AIDS Research Center, National Institute of Infectious Diseases, Tokyo, Japan, **2** The Institute of Medical Science, The University of Tokyo, Tokyo, Japan, **3** DNAVEC Corporation, Tsukuba, Japan, **4** Institute for Virus Research, Kyoto University, Kyoto, Japan, **5** Department of Molecular Pathogenesis, Medical Research Institute, Tokyo Medical and Dental University, Tokyo, Japan

Abstract

Several major histocompatibility complex class I (MHC-I) alleles are associated with lower viral loads and slower disease progression in human immunodeficiency virus (HIV) and simian immunodeficiency virus (SIV) infections. Immune-correlates analyses in these MHC-I-related HIV/SIV controllers would lead to elucidation of the mechanism for viral control. Viral control associated with some protective MHC-I alleles is attributed to CD8$^+$ T-cell responses targeting Gag epitopes. We have been trying to know the mechanism of SIV control in multiple groups of Burmese rhesus macaques sharing MHC-I genotypes at the haplotype level. Here, we found a protective MHC-I haplotype, *90-010-Id* (D), which is not associated with dominant Gag-specific CD8$^+$ T-cell responses. Viral loads in five D$^+$ animals became significantly lower than those in our previous cohorts after 6 months. Most D$^+$ animals showed predominant Nef-specific but not Gag-specific CD8$^+$ T-cell responses after SIV challenge. Further analyses suggested two Nef-epitope-specific CD8$^+$ T-cell responses exerting strong suppressive pressure on SIV replication. Another set of five D$^+$ animals that received a prophylactic vaccine using a Gag-expressing Sendai virus vector showed significantly reduced viral loads compared to unvaccinated D$^+$ animals at 3 months, suggesting rapid SIV control by Gag-specific CD8$^+$ T-cell responses in addition to Nef-specific ones. These results present a pattern of SIV control with involvement of non-Gag antigen-specific CD8$^+$ T-cell responses.

Citation: Takahashi N, Nomura T, Takahara Y, Yamamoto H, Shiino T, et al. (2013) A Novel Protective MHC-I Haplotype Not Associated with Dominant Gag-Specific CD8$^+$ T-Cell Responses in SIVmac239 Infection of Burmese Rhesus Macaques. PLoS ONE 8(1): e54300. doi:10.1371/journal.pone.0054300

Editor: Douglas F. Nixon, University of California San Francisco, United States of America

Received November 13, 2012; **Accepted** December 10, 2012; **Published** January 14, 2013

Funding: This work was supported by grants-in-aid from the Ministry of Education, Culture, Sports, Science, and Technology, and grants-in-aid from the Ministry of Health, Labor, and Welfare. The funders had no role in study design, data collection and analysis, decision to publish, or preparation of the manuscript.

Competing Interests: Makoto Inoue, Akihiro Iida, Hiroto Hara, Tsugumine Shu and Mamoru Hasegawa are employed by DNAVEC Corporation. There are no patents, products in development or marketed products to declare. This does not alter the authors' adherence to all the PLOS ONE policies on sharing data and materials, as detailed online in the guide for authors.

* E-mail: tmatano@nih.go.jp

Introduction

Virus-specific CD8$^+$ T-cell responses play a central role in the control of human immunodeficiency virus (HIV) and simian immunodeficiency virus (SIV) replication [1,2,3,4,5]. Genetic diversities of HLA or major histocompatibility complex class I (MHC-I) result in various patterns of CD8$^+$ T-cell responses in HIV-infected individuals. Cumulative studies on HIV infection have indicated the association of MHC-I genotypes with higher or lower viral loads [6,7,8,9,10]. In some MHC-1 alleles associating with lower viral loads and slower disease progression, certain CD8$^+$ T-cell responses restricted by these MHC-I molecules have been shown to be responsible for HIV control [11,12,13]. In rhesus macaque AIDS models, *Mamu-A*01*, *Mamu-B*08*, and *Mamu-B*17* are known as protective alleles, and macaques possessing these alleles tend to show slower disease progression after SIVmac251/SIVmac239 challenge [14,15,16,17].

Recent studies have indicated great contribution of CD8$^+$ T-cell responses targeting Gag epitopes to reduction in viral loads in HIV/SIV infection [18,19,20,21]. Viral control associated with some protective MHC-I alleles is attributed to Gag epitope-specific CD8$^+$ T-cell responses [22,23,24]. For instance, CD8$^+$ T-cell responses specific for the HLA-B*57-restricted $Gag_{240-249}$ TW10 and HLA-B*27-restricted $Gag_{263-272}$ KK10 epitopes exert strong suppressive pressure on HIV replication and frequently select for an escape mutation with viral fitness costs, leading to lower viral loads [22,24,25,26,27]. On the other hand, CD8$^+$ T-cell responses targeting SIV antigens other than Gag, such as Mamu-B*08- or Mamu-B*17-restricted Vif and Nef epitopes, have been indicated to exert strong suppressive pressure on SIV replication [28,29,30,31,32,33]. Accumulation of our knowledge on the potential of these non-Gag-specific as well as Gag-specific CD8$^+$ T-cell responses for HIV/SIV control should be encouraged for elucidation of viral control mechanisms.

We have been examining SIVmac239 infection in multiple groups of Burmese rhesus macaques sharing MHC-I genotypes at the haplotype level and indicated an association of MHC-I haplotypes with AIDS progression [21,34]. In our previous study, a group of macaques sharing MHC-I haplotype *90-120-Ia* (A) induced dominant Gag-specific $CD8^+$ T-cell responses and tended to show slower disease progression after SIVmac239 challenge [21]. Prophylactic immunization of these A^+ macaques with a DNA vaccine prime and a Gag-expressing Sendai virus (SeV-Gag) vector boost resulted in SIV control based on Gag-specific $CD8^+$

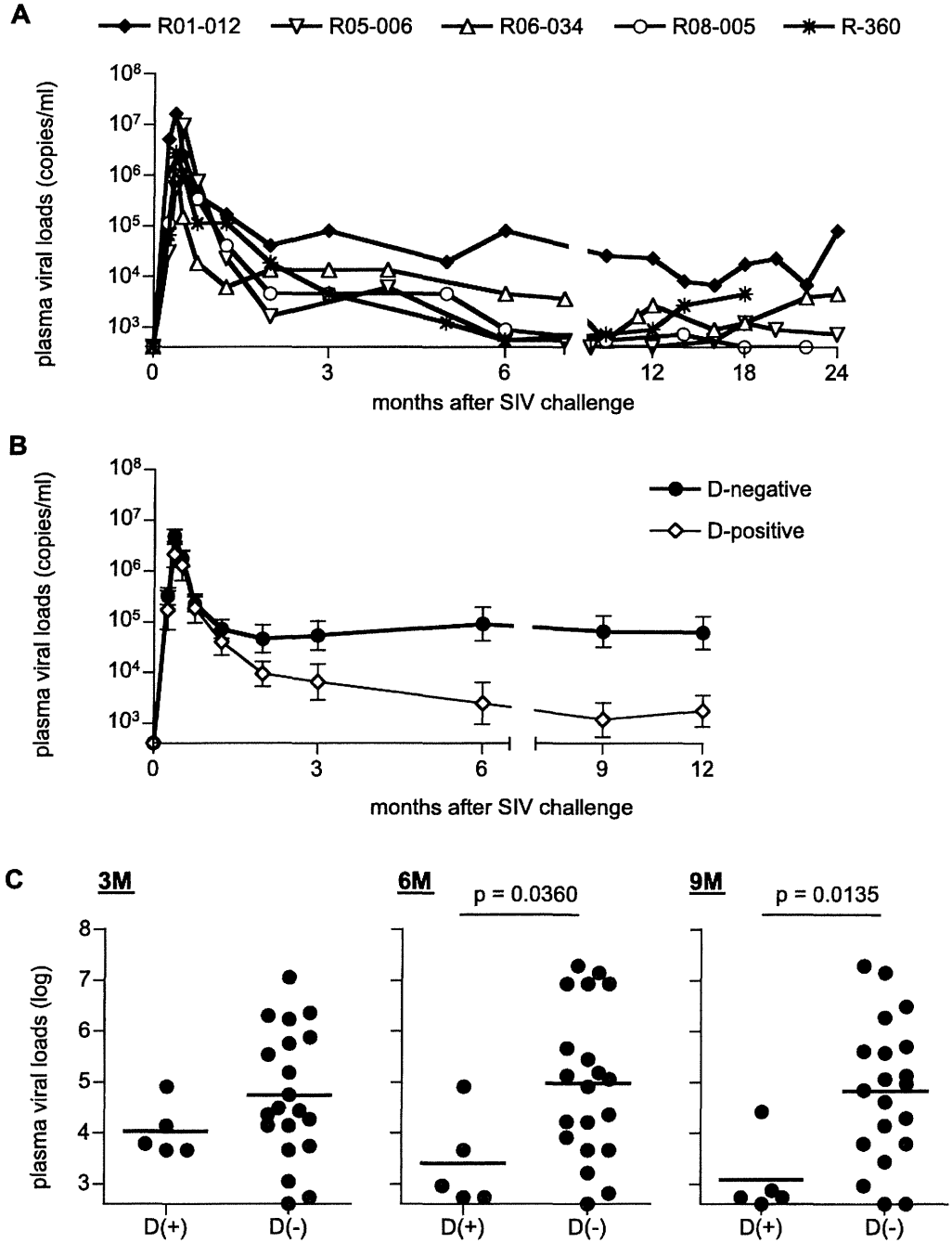

Figure 1. Plasma viral loads after SIVmac239 challenge in unvaccinated macaques. Plasma viral loads (SIV *gag* RNA copies/ml plasma) were determined as described previously [35]. The lower limit of detection is approximately 4×10^2 copies/ml. (A) Changes in plasma viral loads after challenge in unvaccinated macaques possessing MHC-I haplotype D. (B) Changes in geometric means of plasma viral loads after challenge in five unvaccinated D^+ animals in the present study and twenty D^- animals in our previous cohorts [21]. Three of twenty D^- animals were euthanized because of AIDS before 12 months, and we compared viral loads between D^+ and D^- animals until 12 months. (C) Comparison of plasma viral loads at 3 months (left panel), 6 months (middle panel), and 9 months (right panel) between the unvaccinated D^+ and the D^- animals. Viral loads at 6 months and 9 months in D^+ animals were significantly lower than those in the latter D^- animals ($p = 0.0360$ at 6 months and $p = 0.0135$ at 9 months by t-test).

doi:10.1371/journal.pone.0054300.g001

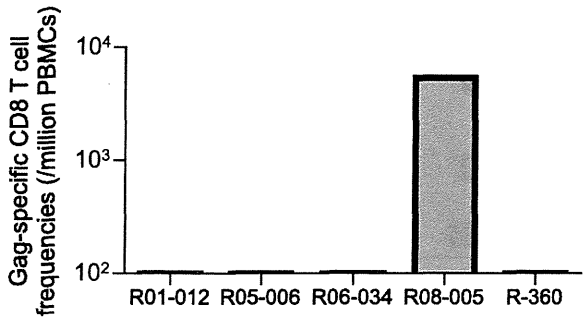

Figure 2. SIV Gag-specific CD8$^+$ T-cell responses in unvaccinated D$^+$ macaques at week 2 after SIVmac239 challenge.
doi:10.1371/journal.pone.0054300.g002

T-cell responses [35,36]. Accumulation of data on interaction between virus replication and T-cell responses in multiple groups of macaques sharing individual MHC-I haplotypes would provide great insights into our understanding of the mechanism for HIV/SIV control.

In the present study, we investigated SIVmac239 infection of a group of Burmese rhesus macaques possessing the MHC-I haplotype *90-010-Id* (D), which was not associated with dominant Gag-specific CD8$^+$ T-cell responses. These animals had persistent viremia in the early phase but showed significant reduction of viral loads around 6 months after SIV challenge. Most D$^+$ animals showed predominant Nef-specific but not Gag-specific CD8$^+$ T-cell responses. This study presents a protective MHC-I haplotype, indicating the potential of non-Gag antigen-specific CD8$^+$ T-cell responses to contribute to SIV control.

Materials and Methods

Ethics Statement

Animal experiments were carried out in National Institute of Biomedical Innovation (NIBP) and Institute for Virus Research in Kyoto University (IVRKU) after approval by the Committee on the Ethics of Animal Experiments of NIBP and IVRKU in accordance with the guidelines for animal experiments at NIBP, IVRKU, and National Institute of Infectious Diseases. To prevent viral transmission, animals were housed in individual cages allowing them to make sight and sound contact with one another, where the temperature was kept at 25°C with light in 12 hours per day. Animals were fed with apples and commercial monkey diet (Type CMK-2, Clea Japan, Inc. Tokyo). Blood collection, vaccination, and SIV challenge were performed under ketamine anesthesia. The endpoint for euthanasia was determined by typical signs of AIDS including reduction in peripheral CD4$^+$ T-cell counts (less than 200 cells/μl), 10% loss of body weight, diarrhea, and general weakness. At euthanasia, animals were deeply anesthetized with pentobarbital under ketamine anesthesia, and then, whole blood was collected from left ventricle.

Animal Experiments

We examined SIV infections in a group of Burmese rhesus macaques (n = 10) sharing the MHC-I haplotype *90-010-Id* (D). The determination of MHC-I haplotypes was based on the family study in combination with the reference strand-mediated conformation analysis (RSCA) of *Mamu-A* and *Mamu-B* genes and detection of major *Mamu-A* and *Mamu-B* alleles by cloning the reverse transcription (RT)-PCR products as described previously [21,34,37]. Macaques R01-012 and R01-009 used in our previous report [35] and macaques R03-021 and R03-016 used in an unpublished experiment were included in the present study. Five macaques R01-009, R06-020, R06-033, R03-021, and R03-016 received a prophylactic DNA prime/SeV-Gag boost vaccine (referred to as DNA/SeV-Gag vaccine) [35]. The DNA used for the vaccination, CMV-SHIVdEN, was constructed from an *env*-deleted and *nef*-deleted simian–human immunodeficiency virus SHIVMD14YE [38] molecular clone DNA (SIVGP1) and has the genes encoding SIVmac239 Gag, Pol, Vif, and Vpx, and HIV Tat and Rev. At the DNA vaccination, animals received 5 mg of CMV-SHIVdEN DNA intramuscularly. Six weeks after the DNA prime, animals received a single boost intranasally with 6×10^9 cell infectious units (CIUs) of F-deleted replication-defective SeV-Gag [39,40]. All animals were challenged intravenously with 1,000 $TCID_{50}$ (50 percent tissue culture infective doses) of SIVmac239 [41]. At week 1 after SIV challenge, macaque R03-021 was inoculated with nonspecific immunoglobulin G (IgG) and macaques R03-016 with IgG purified from neutralizing antibody-positive plasma of chronically SIV-infected macaques in our previous experiment [42].

Analysis of SIV Antigen-specific CD8$^+$ T-cell Responses

SIV antigen-specific CD8$^+$ T-cell responses were measured by flow-cytometric analysis of gamma interferon (IFN-γ) induction as described previously [43]. Autologous herpesvirus papio-immortalized B-lymphoblastoid cell lines (B-LCLs) were established from peripheral blood mononuclear cells (PBMCs) which were obtained from individual macaques before SIV challenge [44]. PBMCs obtained from SIV-infected macaques were cocultured with autologous B-LCLs pulsed with peptides or peptide pools using panels of overlapping peptides spanning the entire SIVmac239 Gag, Pol, Vif, Vpx, Vpr, Tat, Rev, Env, and Nef amino acid sequences. Alternatively, PBMCs were cocultured with B-LCLs infected with a vaccinia virus vector expressing SIVmac239 Gag for Gag-specific stimulation. Intracellular IFN-γ staining was performed using CytofixCytoperm kit (BD, Tokyo, Japan). Fluorescein isothiocianate-conjugated anti-human CD4 (BD), Peridinin chlorophyll protein (PerCP)-conjugated anti-human CD8 (BD), allophycocyanin Cy7 (APC-Cy7)-conjugated anti-human CD3 (BD), and phycoerythrin (PE)-conjugated anti-human IFN-γ antibodies (Biolegend, San Diego, CA) were used. Specific T-cell levels were calculated by subtracting non-specific IFN-γ$^+$ T-cell frequencies from those after peptide-specific stimulation. Specific T-cell levels less than 100 cells per million PBMCs were considered negative.

Sequencing Analysis of Plasma Viral Genomes

Viral RNAs were extracted using High Pure Viral RNA kit (Roche Diagnostics, Tokyo, Japan) from macaque plasma samples. Fragments of cDNAs encoding SIVmac239 Gag and Nef were amplified by nested RT-PCR from plasma RNAs and subjected to direct sequencing by using dye terminator chemistry and an automated DNA sequencer (Applied Biosystems, Tokyo, Japan) as described before [45]. Predominant non-synonymous mutations were determined.

Statistical Analysis

Statistical analysis was performed using Prism software version 4.03 with significance levels set at a P value of <0.050 (GraphPad Software, Inc., San Diego, CA). Plasma viral loads were log transformed and compared by an unpaired two-tailed t test.

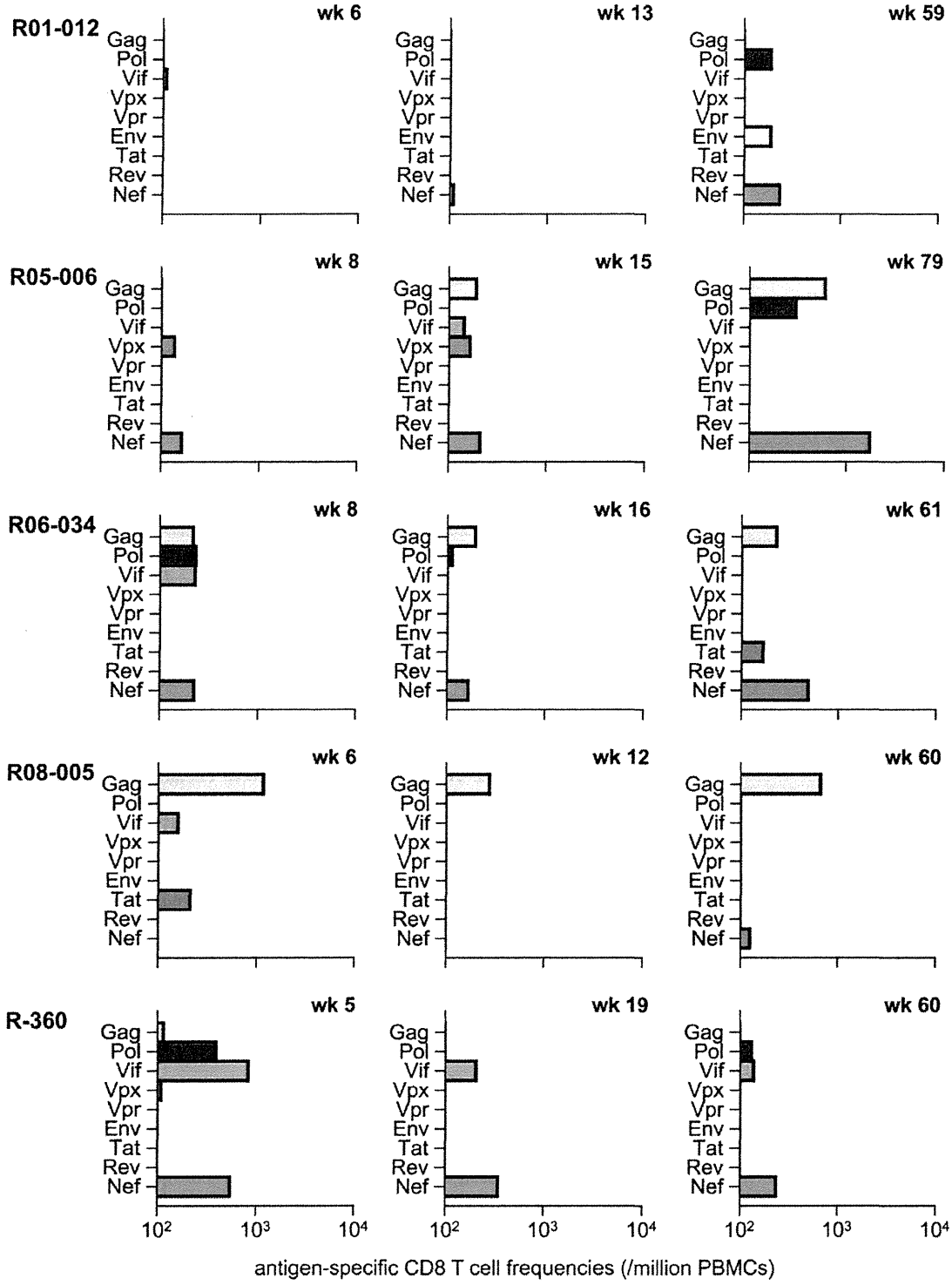

Figure 3. SIV antigen-specific CD8$^+$ T-cell responses in unvaccinated D$^+$ macaques. Responses were measured by the detection of antigen-specific IFN-γ induction in PBMCs obtained at indicated time points after SIVmac239 challenge.
doi:10.1371/journal.pone.0054300.g003

Results

Lower Viral Loads in D$^+$ Macaques in the Chronic Phase of SIV Infection

We first investigated SIVmac239 infection of five unvaccinated Burmese rhesus macaques sharing the MHC-I haplotype D (referred to as D$^+$ macaques). Confirmed MHC-I alleles consisting of this haplotype is *Mamu-A1*032:02*, *Mamu-B*004:01*, and *Mamu-B*102:01:01*. These animals showed lower set-point plasma viral loads (Fig. 1). Comparison of plasma viral loads between these five animals and our previous cohorts of SIVmac239-infected Burmese D-negative (D$^-$) rhesus macaques (n = 20) [21] revealed no

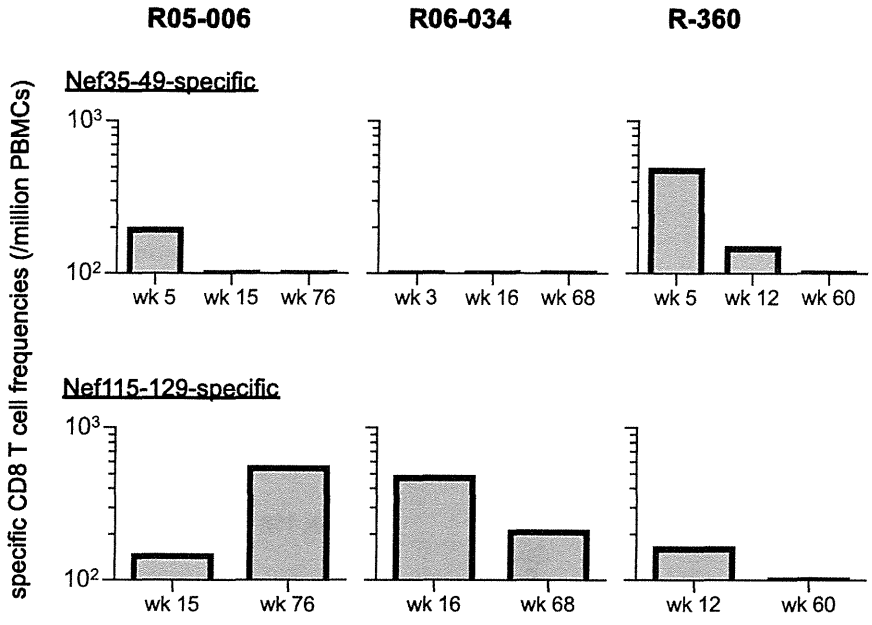

Figure 4. SIV Nef-specific CD8$^+$ T-cell responses in macaques R05-006, R06-034, and R-360. Nef_{35-49}-specific (upper panels) and $Nef_{115-129}$-specific (lower panels) CD8$^+$ T-cell responses were examined at indicated time points after SIVmac239 challenge.
doi:10.1371/journal.pone.0054300.g004

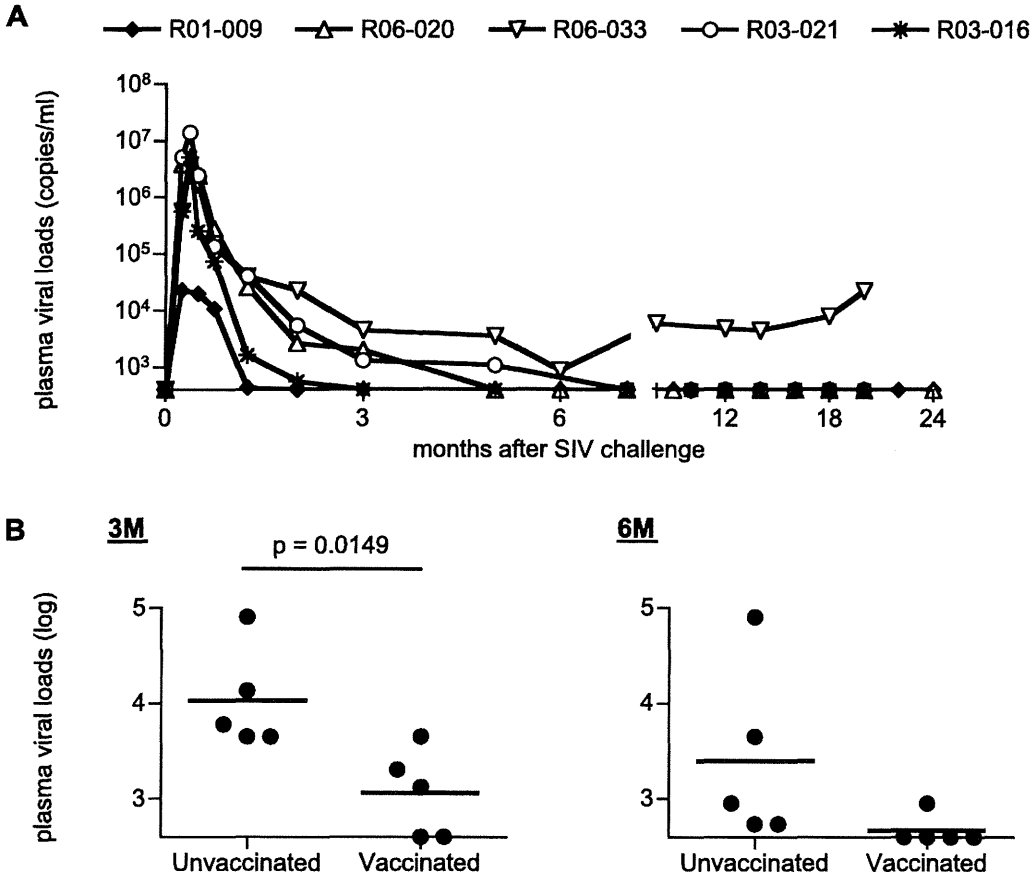

Figure 5. Plasma viral loads after SIVmac239 challenge in vaccinated D$^+$ macaques. (A) Changes in plasma viral loads after challenge vaccinated macaques possessing MHC-I haplotype D. (B) Comparison of plasma viral loads at 3 months (left panel) and 6 months (right panel) between five unvaccinated D$^+$ and five vaccinated D$^+$ animals. Viral loads at 3 months in vaccinated animals were significantly lower than those in the unvaccinated ($p = 0.0149$ by t-test).
doi:10.1371/journal.pone.0054300.g005

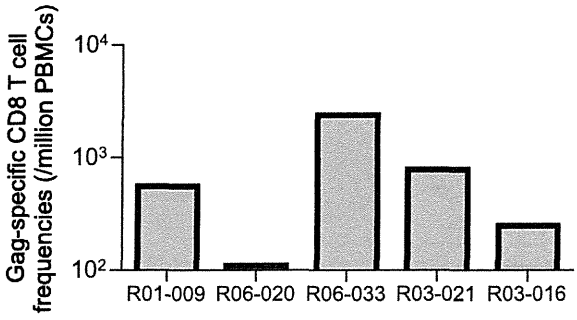

Figure 6. SIV Gag-specific CD8$^+$ T-cell responses in vaccinated D$^+$ macaques at week 2 after SIVmac239 challenge.
doi:10.1371/journal.pone.0054300.g006

significant difference at 3 months after SIV challenge ($p = 0.2436$ by t-test), but viral loads in the former D$^+$ animals became significantly lower than the latter after 6 months ($p = 0.0360$ at 6 months and $p = 0.0135$ at 9 months by t-test; Fig. 1). Four of these five macaques sharing MHC-I haplotype D showed low viral loads, less than 5×10^3 copies/ml, after 6 months, whereas macaque R01-012 maintained relatively higher viral loads.

Predominant Nef-specific CD8$^+$ T-cell Responses

We examined SIV antigen-specific CD8$^+$ T-cell responses by detection of antigen-specific IFN-γ induction. In the very acute phase, we did not have enough PBMC samples for measurement of individual SIV antigen-specific CD8$^+$ T-cell responses and focused on examining Gag-specific CD8$^+$ T-cell responses in most animals. At week 2 after challenge, Gag-specific CD8$^+$ T-cell responses were undetectable in four of five animals (Fig. 2).

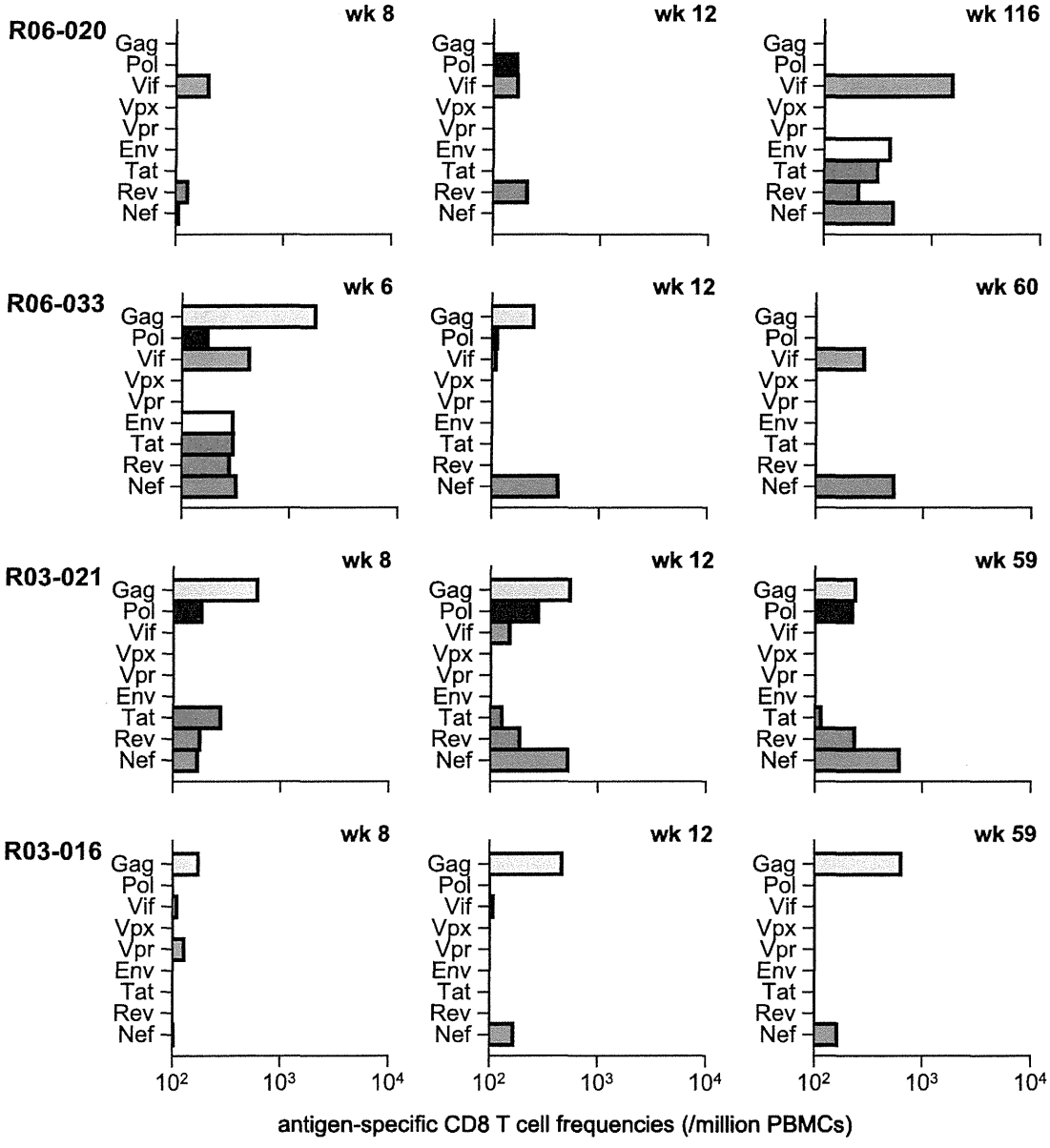

Figure 7. SIV antigen-specific CD8$^+$ T-cell responses in vaccinated D$^+$ animals after SIVmac239 challenge. Samples for this analysis were unavailable in macaque R01-009.
doi:10.1371/journal.pone.0054300.g007

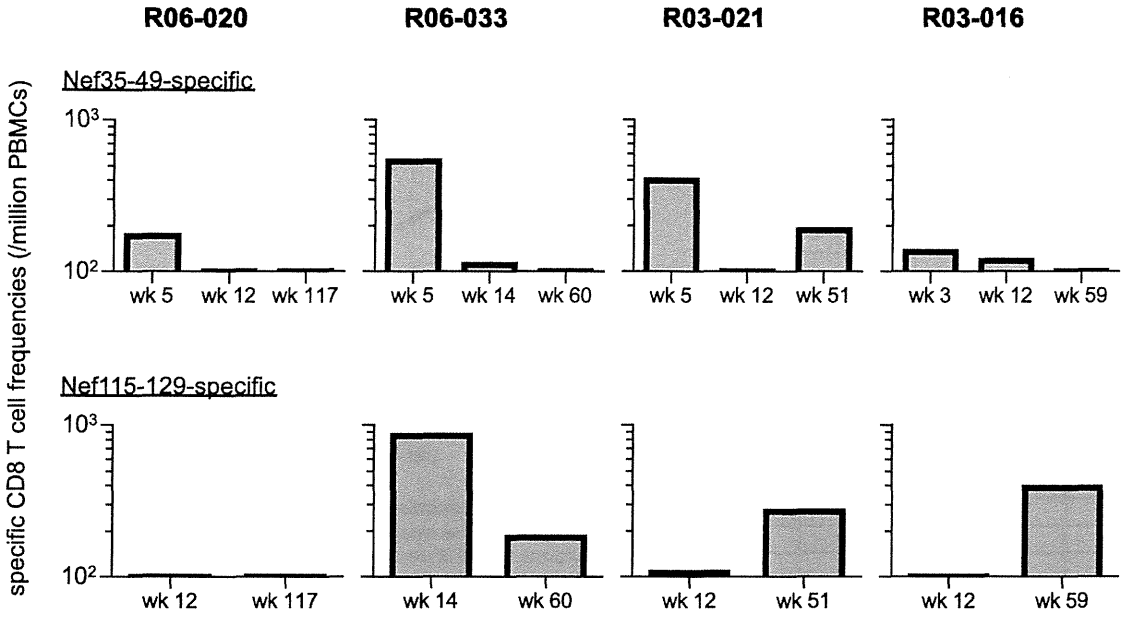

Figure 8. SIV Nef-specific CD8$^+$ T-cell responses in macaques R06-020, R06-033, R03-021, and R03-016. Nef_{35-49}-specific (upper panels) and $Nef_{115-129}$-specific (lower panels) CD8$^+$ T-cell responses were examined at indicated time points after SIVmac239 challenge.
doi:10.1371/journal.pone.0054300.g008

We then examined CD8$^+$ T-cell responses specific for individual SIV antigens in the early and the late phases (Fig. 3). Nef-specific but not Gag-specific CD8$^+$ T-cell responses were predominant in most D$^+$ animals. Gag-specific CD8$^+$ T-cell responses were dominantly induced in macaque R08-005 showing very low set-point viral loads. Macaque R01-012 having higher viral loads showed poor CD8$^+$ T-cell responses in the early phase.

Among four D$^+$ animals controlling SIV replication with less than 5×10^3 copies/ml of plasma viral loads after 6 months, Gag-specific CD8$^+$ T-cell responses were dominant only in macaque R08-005, while efficient Nef-specific CD8$^+$ T-cell responses were induced in the remaining three, suggesting possible contribution of Nef-specific CD8$^+$ T-cell responses to SIV control in these three controllers (R05-006, R06-034, and R-360). We then attempted to localize Nef CD8$^+$ T-cell epitopes shared in these animals and found Nef_{35-49}-specific and $Nef_{115-129}$-specific CD8$^+$ T-cell responses (Fig. 4), although we did not have enough samples for mapping the exact epitopes.

Reduction of Viral Loads in the Early Phase of SIV Infection by Prophylactic Vaccination

We also investigated SIVmac239 infection of additional five, vaccinated Burmese rhesus macaques sharing the MHC-I haplotype D. These animals received a prophylactic DNA/SeV-Gag vaccination. In four of these five vaccinated macaques, plasma viremia became undetectable after 6 months, while macaque R06-033 showed persistent viremia (Fig. 5A). Difference in viral loads between unvaccinated and vaccinated D$^+$ animals was unclear in the acute phase, but the latter vaccinees showed significant reduction in viral loads compared to those in the former unvaccinated at 3 months ($p = 0.0360$; Fig. 5B). After 6 months, unvaccinated animals also showed reduced viral loads, and the difference in viral loads between unvaccinated and vaccinated became unclear.

In contrast to unvaccinated D$^+$ animals, all five vaccinated animals elicited Gag-specific CD8$^+$ T-cell responses at week 2 after challenge (Fig. 6), reflecting the effect of prophylactic vaccination. We then examined CD8$^+$ T-cell responses specific for individual SIV antigens in these vaccinated animals (Fig. 7). Samples for this analysis were unavailable in vaccinated macaque R01-009. Vaccinated animals except for macaque R06-020 showed dominant Gag-specific CD8$^+$ T-cell responses even at 1–2 months. However, Gag-specific CD8$^+$ T-cell responses became not dominant after 1 year, while Nef-specific or Vif-specific CD8$^+$ T-cell responses became predominant, instead, in most vaccinees except for macaque R03-016.

Like three unvaccinated macaques (R05-006, R06-034, and R-360), vaccinated D$^+$ animals induced Nef_{35-49}-specific and $Nef_{115-129}$-specific CD8$^+$ T-cell responses after SIV challenge (Fig. 8). In analyses of three unvaccinated (Fig. 4) and four vaccinated animals (Fig. 8), Nef_{35-49}-specific CD8$^+$ T-cell responses were induced in the early phase in six animals but mostly became undetectable in the chronic phase. $Nef_{115-129}$-specific CD8$^+$ T-cell responses were also induced in most animals except for macaque R06-020 which showed $Nef_{112-126}$-specific ones in the chronic phase (data not shown). Macaques R05-006, R03-021, and R03-016 showed efficient $Nef_{115-129}$-specific CD8$^+$ T-cell responses not in the early phase but in the chronic phase. In contrast, vaccinated animal R06-033 that failed to control viremia showed higher $Nef_{115-129}$-specific CD8$^+$ T-cell responses in the early phase than those in the chronic phase.

Selection of Mutations in Nef CD8$^+$ T-cell Epitope-coding Regions

To see the effect of selective pressure by Nef-specific CD8$^+$ T-cell responses on viral genome mutations, we next analyzed nucleotide sequences in viral *nef* cDNAs amplified from plasma RNAs obtained at several time points after SIV challenge. Nonsynonymous mutations detected predominantly in Nef_{35-49}-coding and $Nef_{115-129}$-coding regions were as shown in Fig. 9. Remarkably, all the unvaccinated and vaccinated D$^+$ animals showed rapid selection of mutations in the Nef_{35-49}-coding region in 3 months. On the other hand, mutations in the $Nef_{115-129}$-coding region were observed in the late phase in all the three

		Nef35-49						Nef115-129				
Nef		36	37	41	42	44		119	122	124	125	126
		E	D	Q	S	G		M	F	K	E	K
R01-012	1M		*G									
	3M		*G									
	14M	*G	*G									
	24M	*G	*G			*E						
R05-006	1M					*E						
	3M			R								
	16M			R								
	24M			R								R
R06-034	1M											
	3M	*G										
	10M	*G	*G			*E						*R
	18M	G				E						R
R08-005	1M											
	3M				*F							
	6M	G										
	14M				F							
	24M	*G			F							
R-360	1M											
	3M		*G									
	6M		G									
	12M		G					T	L			
	20M		G					T	L			
R06-020	1M											
	3M	*K										
	11M		G	R								
R06-033	1M											
	3M	*G										
	6M		*G									
	14M		G			*E					K	E
R03-021	1M											
	3M				*F							
	14M	G								R		
R03-016	1M	*K		*R								
	4M	K										
	12M	K										

Figure 9. Predominant non-synonymous mutations in Nef_{35-49}-coding and $Nef_{115-129}$-coding regions of viral cDNAs in D^+ animals after SIVmac239 challenge. Amino acid substitutions are shown. Detection of similar levels of wild-type and mutant sequences at the residue is indicated by asterisks. Samples for this analysis were unavailable in macaque R01-009.
doi:10.1371/journal.pone.0054300.g009

unvaccinated animals eliciting $Nef_{115-129}$-specific $CD8^+$ T-cell responses. These mutations were also detected in two of three vaccinated animals eliciting $Nef_{115-129}$-specific $CD8^+$ T-cell responses.

We also analyzed viral *gag* sequences to see the effect of Gag-specific $CD8^+$ T-cell pressure on viral genome mutations in vaccinated animals (data not shown). Our previous study [35] showed rapid selection of a mutation leading to a glutamine (Q)-to-lysine (K) change at the 58th residue in Gag (Q58K) at week 5 in vaccinated macaque R01-009, although no more samples were available for this sequencing analysis. This Q58K mutation results in escape from Gag_{50-65}-specific $CD8^+$ T-cell recognition. In the present study, macaque R03-016 showed rapid selection of a mutation leading to a K-to-asparagine (N) change at the 478th residue in Gag in 1 month. These results may reflect rapid disappearance of detectable plasma viremia in 1 or 2 months in these two vaccinees. Macaque R06-020 showed selection of a *gag* mutation in 3 months, while other two vaccinees (R06-033 and R03-021) selected no *gag* mutation in the early phase.

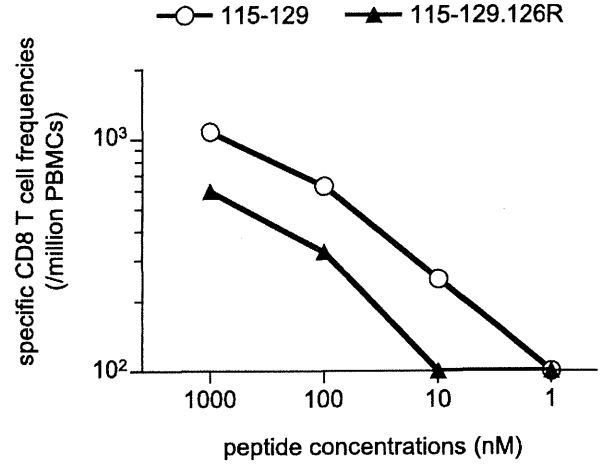

Figure 10. IFN-γ induction in $CD8^+$ T cells after stimulation with the wild-type or the mutant peptide. PBMCs obtained at week 31 from macaque R06-033 were stimulated by coculture with B-LCL pulsed with indicated concentrations of the wild-type $Nef_{115-129}$ peptide (open circles, 115–129, LAIDMSHFIKEKGGL) or the mutant $Nef_{115-129}$ peptide with a K126R alteration (closed triangles, 115–129.126R, LAIDMSHFIKERGGL).
doi:10.1371/journal.pone.0054300.g010

Discussion

HIV infection in humans with polymorphic MHC-I genotypes induces various patterns of viral antigen-specific $CD8^+$ T-cell responses. Previous studies have found several protective MHC-I alleles associated with lower viral loads and slower disease progression in HIV/SIV infection [7,13,14,16,17]. Elucidation of the mechanisms of viral control associated with individual protective MHC-I alleles would contribute to HIV cure and vaccine-based prevention. Because $CD8^+$ T-cell responses specific for some MHC-I-restricted epitopes can be affected by those specific for other MHC-I-restricted epitopes due to immunodominance [29,46,47], macaque groups sharing MHC-I genotypes at the haplotype level are useful for the analysis of cooperation of multiple epitope-specific $CD8^+$ T-cell responses. Previously, we reported a group of Burmese rhesus macaques sharing MHC-I haplotype *90-120-Ia* (A), which dominantly induce Gag-specific $CD8^+$ T-cell responses and tend to show slower disease progression after SIVmac239 challenge [21]. In the present study, we presented another type of protective MHC-I haplotype, which is not associated with dominant Gag-specific $CD8^+$ T-cell responses. Significant reduction of viral loads in unvaccinated macaques possessing this D haplotype compared to those in D^- macaques was observed after 6 months. Analysis of SIV infection in macaques sharing this protective MHC-I haplotype would lead to understanding of $CD8^+$ T-cell cooperation for viral control.

Analyses of antigen-specific $CD8^+$ T-cell responses after SIVmac239 challenge indicate that this MHC-I haplotype D is associated with predominant Nef-specific $CD8^+$ T-cell responses. Nef-specific $CD8^+$ T-cell responses were efficiently induced in all SIV controllers, whereas Gag-specific $CD8^+$ T-cell responses were dominant in only one of them. We found Nef_{35-49}-specific and $Nef_{115-129}$-specific $CD8^+$ T-cell responses shared in D^+ animals. We were unable to determine the MHC-I alleles restricting these epitopes, but these responses are not usually induced in our

previous D^- cohorts and considered to be associated with this MHC-I haplotype D.

Sequencing analysis of viral genomes showed rapid selection of mutations in the Nef_{36-44}-coding region within 3 months in all the D^+ animals. This is consistent with our results that Nef_{35-49}-specific $CD8^+$ T-cell responses were mostly induced in the early phase but undetectable in the chronic phase. These mutations were not consistently selected in our previous D^- cohorts and thus considered as MHC-I haplotype D-associated mutations. This suggests strong selective pressure by Nef_{35-49}-specific $CD8^+$ T-cell responses in the acute phase of SIVmac239 infection in D^+ macaques, although it remains undetermined whether these mutations result in viral escape from Nef_{35-49}-specific $CD8^+$ T-cell recognition.

$Nef_{115-129}$-specific $CD8^+$ T-cell responses were detected in six D^+ animals. In five of them, nonsynonymous mutations in the $Nef_{119-126}$-coding region were observed in the chronic phase. At least, we confirmed viral escape from $Nef_{115-129}$-specific $CD8^+$ T-cell recognition by a mutation leading to a K-to-arginine (R) (K126R) substitution at Nef residue 126 (Fig. 10). The number of nonsynonymous substitutions per the number of sites estimated to be nonsynonymous (dN) exceeded that estimated to be synonymous (dS) during the evolution process of $Nef_{115-129}$-coding region, but the value did not show statistically significant difference from that of neutral selection. Among three unvaccinated animals that controlled SIV replication without dominant Gag-specific $CD8^+$ T-cell responses, amino acid substitutions in the $Nef_{119-126}$-coding region were observed in a year in macaques R06-034 and R-360 but after 2 years in macaque R05-006. The former two animals tended to show earlier increases in plasma viral loads in the chronic phase, while the latter R05-006 maintained higher frequencies of $Nef_{115-129}$-specific $CD8^+$ T-cell responses. $Nef_{115-129}$-specific $CD8^+$ T-cell responses were efficient in the chronic phase in vaccinated controllers R03-021 and R03-016 but decreased in R06-033 that failed to contain SIV replication. Although a possible effect of this haplotype-associated factors other than $CD8^+$ T-cell responses such as NK activity on SIV infection [48,49,50] remains undetermined, these results imply involvement of Nef-specific $CD8^+$ T-cell responses in the SIV control associated with MHC-I haplotype D.

Unvaccinated macaque R08-005 dominantly elicited Gag antigen-specific $CD8^+$ T-cell responses and showed rapid selection of a mutation encoding Gag 257 residue, which was not observed in any other D^+ animals. Nef-specific $CD8^+$ T-cell responses were detectable only at week 2 in the acute phase (data not shown) and a mutation in the Nef_{42}-coding region was rapidly selected. It is speculated that those dominant Gag-specific $CD8^+$ T-cell responses associated with the second, non-D MHC-I haplotype were effective in this animal. Nef_{35-49}-specific $CD8^+$ T-cell responses may not be efficient due to immunodominance but exert some suppressive pressure on viral replication.

DNA/SeV-Gag vaccination resulted in earlier reduction of viral loads after SIV challenge. Vaccinees showed significantly lower viral loads at 3 months than those in unvaccinated animals. Gag-specific $CD8^+$ T-cell responses were elicited at week 2 in all the vaccinees but not in the unvaccinated except for one animal R08-005. No *gag* mutations were shared in the vaccinees in the acute phase, but three of them showed rapid selection of individual non-synonymous mutations in *gag*. Rapid selection of mutations in the Nef_{36-44}-coding region was consistently detected even in these vaccinees. These results suggest broader $CD8^+$ T-cell responses consisting of dominant vaccine antigen Gag-specific and inefficient naive-derived Nef-specific ones in the acute phase. In three vaccinated animals, Gag-specific $CD8^+$ T-cell responses became lower or undetectable, and instead, Nef-specific $CD8^+$ T-cell responses became predominant in the chronic phase.

In summary, we found a protective MHC-I haplotype not associated with dominant Gag-specific $CD8^+$ T-cell responses in SIVmac239 infection. Our results in D^+ macaques suggest suppressive pressure by Nef_{35-49}-specific and $Nef_{115-129}$-specific $CD8^+$ T-cell responses on SIV replication, contributing to reduction in set-point viral loads. DNA/SeV-Gag-vaccinated D^+ animals induced Gag-specific $CD8^+$ T-cell responses in addition to Nef-specific ones after SIV challenge, resulting in earlier containment of SIV replication. This study presents a pattern of SIV control with involvement of non-Gag antigen-specific $CD8^+$ T-cell responses, contributing to accumulation of our knowledge on HIV/SIV control mechanisms.

Acknowledgments

We thank F. Ono, K. Oto, K. Hanari, K. Komatsuzaki, M. Hamano, H. Akari, and Y. Yasutomi for their assistance in animal experiments.

Author Contributions

Performed animal experiments: HS TM TI YK. Performed MHC-I typing: TKN AK. Conceived and designed the experiments: NT TM. Performed the experiments: NT TN YT HY AT. Analyzed the data: NT HY T. Shiino TM. Contributed reagents/materials/analysis tools: MI AI HH T. Shu MH. Wrote the paper: NT TM.

References

1. Borrow P, Lewicki H, Hahn BH, Shaw GM, Oldstone MB (1994) Virus-specific CD8+ cytotoxic T-lymphocyte activity associated with control of viremia in primary human immunodeficiency virus type 1 infection. J Virol 68: 6103–6110.
2. Koup RA, Safrit JT, Cao Y, Andrews CA, McLeod G, et al. (1994) Temporal association of cellular immune responses with the initial control of viremia in primary human immunodeficiency virus type 1 syndrome. J Virol 68: 4650–4655.
3. Matano T, Shibata R, Siemon C, Connors M, Lane HC, et al. (1998) Administration of an anti-CD8 monoclonal antibody interferes with the clearance of chimeric simian/human immunodeficiency virus during primary infections of rhesus macaques. J Virol 72: 164–169.
4. Jin X, Bauer DE, Tuttleton SE, Lewin S, Gettie A, et al. (1999) Dramatic rise in plasma viremia after CD8+ T cell depletion in simian immunodeficiency virus-infected macaques. J Exp Med 189: 991–998.
5. Schmitz JE, Kuroda MJ, Santra S, Sasseville VG, Simon MA, et al. (1999) Control of viremia in simian immunodeficiency virus infection by CD8+ lymphocytes. Science 283: 857–860.
6. Carrington M, Nelson GW, Martin MP, Kissner T, Vlahov D, et al. (1999) HLA and HIV-1: heterozygote advantage and B*35-Cw*04 disadvantage. Science 283: 1748–1752.
7. Migueles SA, Sabbaghian MS, Shupert WL, Bettinotti MP, Marincola FM, et al. (2000) HLA B*5701 is highly associated with restriction of virus replication in a subgroup of HIV-infected long term nonprogressors. Proc Natl Acad Sci USA 97: 2709–2714.
8. Tang J, Tang S, Lobashevsky E, Myracle AD, Fideli U, et al. (2002) Favorable and unfavorable HLA class I alleles and haplotypes in Zambians predominantly infected with clade C human im- munodeficiency virus type 1. J Virol 76: 8276–8284.
9. Kiepiela P, Leslie AJ, Honeyborne I, Ramduth D, Thobakgale C, et al. (2004) Dominant influence of HLA-B in mediating the potential co-evolution of HIV and HLA. Nature 432: 769–775.
10. Leslie A, Matthews PC, Listgarten J, Carlson JM, Kadie C, et al. (2010) Additive contribution of HLA class I alleles in the immune control of HIV-1 infection. J Virol 84: 9879–9888.
11. Altfeld M, Addo MM, Rosenberg ES, Hecht FM, Lee PK, et al. (2003) Influence of HLA-B57 on clinical presentation and viral control during acute HIV-1 infection. AIDS 17: 2581–2591.
12. Altfeld M, Kalife ET, Qi Y, Streeck H, Lichterfeld M, et al. (2006) HLA alleles associated with delayed progression to AIDS contribute strongly to the initial CD8+ T cell response against HIV-1. PLoS Med 3: e403.
13. Goulder PJ, Watkins DI (2008) Impact of MHC class I diversity on immune control of immunodeficiency virus replication. Nat Rev Immunol 8: 619–630.

14. Muhl T, Krawczak M, Ten Haaft P, Hunsmann G, Sauermann U (2002) MHC class I alleles influence set-point viral load and survival time in simian immunodeficiency virus-infected rhesus monkeys. J Immunol 169: 3438–3446.
15. Mothe BR, Weinfurter J, Wang C, Rehrauer W, Wilson N, et al. (2003) Expression of the major histocompatibility complex class I molecule Mamu-A*01 is associated with control of simian immunodeficiency virus SIVmac239 replication. J Virol 77: 2736–2740.
16. Yant LJ, Friedrich TC, Johnson RC, May GE, Maness NJ, et al. (2006) The high-frequency major histocompatibility complex class I allele Mamu-B*17 is associated with control of simian immunodeficiency virus SIVmac239 replication. J Virol 80: 5074–5077.
17. Loffredo JT, Maxwell J, Qi Y, Glidden CE, Borchardt GJ, et al. (2007) Mamu-B*08-positive macaques control simian immunodeficiency virus replication. J Virol 81: 8827–8832.
18. Edwards BH, Bansal A, Sabbaj S, Bakari J, Mulligan MJ, et al. (2002) Magnitude of functional CD8+ T-cell responses to the gag protein of human immunodeficiency virus type 1 correlates inversely with viral load in plasma. J Virol 76: 2298–2305.
19. Zuniga R, Lucchetti A, Galvan P, Sanchez S, Sanchez C, et al. (2006) Relative dominance of Gag p24-specific cytotoxic T lymphocytes is associated with human immunodeficiency virus control. J Virol 80: 3122–3125.
20. Kiepiela P, Ngumbela K, Thobakgale C, Ramduth D, Honeyborne I, et al. (2007) CD8+ T-cell responses to different HIV proteins have discordant associations with viral load. Nat Med 13: 46–53.
21. Nomura T, Yamamoto H, Shiino T, Takahashi N, Nakane T, et al. (2012) Association of major histocompatibility complex class I haplotypes with disease progression after simian immunodeficiency virus challenge in Burmese rhesus macaques. J Virol 86: 6481–6490.
22. Schneidewind A, Brockman MA, Yang R, Adam RI, Li B, et al. (2007) Escape from the dominant HLA-B27-restricted cytotoxic T-lymphocyte response in Gag is associated with a dramatic reduction in human immunodeficiency virus type 1 replication. J Virol 81: 12382–12393.
23. Emu B, Sinclair E, Hatano H, Ferre A, Shacklett B, et al. (2008) HLA class I-restricted T-cell responses may contribute to the control of human immunodeficiency virus infection, but such responses are not always necessary for long-term virus control. J Virol 82: 5398–5407.
24. Miura T, Brockman MA, Schneidewind A, Lobritz M, Pereyra F, et al. (2009) HLA-B57/B*5801 human immunodeficiency virus type 1 elite controllers select for rare gag variants associated with reduced viral replication capacity and strong cytotoxic T-lymphocyte recognition. J Virol 83: 2743–2755.
25. Leslie AJ, Pfafferott KJ, Chetty P, Draenert R, Addo MM, et al. (2004) HIV evolution: CTL escape mutation and reversion after transmission. Nat Med 10: 282–289.
26. Martinez-Picado J, Prado JG, Fry EE, Pfafferott K, Leslie A, et al. (2006) Fitness cost of escape mutations in p24 Gag in association with control of human immunodeficiency virus type 1. J Virol 80: 3617–3623.
27. Crawford H, Prado JG, Leslie A, Hue S, Honeyborne I, et al. (2007) Compensatory mutation partially restores fitness and delays reversion of escape mutation within the immunodominant HLA-B*5703-restricted Gag epitope in chronic human immunodeficiency virus type 1 infection. J Virol 81: 8346–8351.
28. Friedrich TC, Valentine LE, Yant LJ, Rakasz EG, Piaskowski SM, et al. (2007) Subdominant CD8+ T-cell responses are involved in durable control of AIDS virus replication. J Virol 81: 3465–3476.
29. Loffredo JT, Bean AT, Beal DR, Leon EJ, May GE, et al. (2008) Patterns of CD8+ immunodominance may influence the ability of Mamu-B*08-positive macaques to naturally control simian immunodeficiency virus SIVmac239 replication. J Virol 82: 1723–1738.
30. Maness NJ, Yant LJ, Chung C, Loffredo JT, Friedrich TC, et al. (2008) Comprehensive immunological evaluation reveals surprisingly few differences between elite controller and progressor Mamu-B*17-positive simian immunodeficiency virus-infected rhesus macaques. J Virol 82: 5245–5254.
31. Valentine LE, Loffredo JT, Bean AT, Leon EJ, MacNair CE, et al. (2009) Infection with "escaped" virus variants impairs control of simian immunodeficiency virus SIVmac239 replication in Mamu-B*08-positive macaques. J Virol 83: 11514–11527.
32. Budde ML, Greene JM, Chin EN, Ericsen AJ, Scarlotta M, et al. (2012) Specific CD8+ T cell responses correlate with control of simian immunodeficiency virus replication in Mauritian cynomolgus macaques. J Virol 86: 7596–7604.
33. Mudd PA, Martins MA, Ericsen AJ, Tully DC, Power KA, et al. (2012) Vaccine-induced CD8+ T cells control AIDS virus replication. Nature 491: 129–133.
34. Naruse TK, Chen Z, Yanagida R, Yamashita T, Saito Y, et al. (2010) Diversity of MHC class I genes in Burmese-origin rhesus macaques. Immunogenetics 62: 601–611.
35. Matano T, Kobayashi M, Igarashi H, Takeda A, Nakamura H, et al. (2004) Cytotoxic T lymphocyte-based control of simian immunodeficiency virus replication in a preclinical AIDS vaccine trial. J Exp Med 199: 1709–1718.
36. Kawada M, Tsukamoto T, Yamamoto H, Iwamoto N, Kurihara K, et al. (2008) Gag-specific cytotoxic T-lymphocyte-based control of primary simian immunodeficiency virus replication in a vaccine trial. J Virol 82: 10199–10206.
37. Tanaka-Takahashi Y, Yasunami M, Naruse T, Hinohara K, Matano T, et al. (2007) Reference strand-mediated conformation analysis-based typing of multiple alleles in the rhesus macaque MHC class I Mamu-A and Mamu-B loci. Electrophoresis 28: 918–924.
38. Shibata R, Maldarelli F, Siemon C, Matano T, Parta M, et al. (1997) Infection and pathogenicity of chimeric simian-human immunodeficiency viruses in macaques: determinants of high virus loads and CD4 cell killing. J Infect Dis 176: 362–373.
39. Li HO, Zhu YF, Asakawa M, Kuma H, Hirata T, et al. (2000) A cytoplasmic RNA vector derived from nontransmissible Sendai virus with efficient gene transfer and expression. J Virol 74: 6564–6569.
40. Takeda A, Igarashi H, Nakamura H, Kano M, Iida A, et al. (2003) Protective efficacy of an AIDS vaccine, a single DNA priming followed by a single booster with a recombinant replication-defective Sendai virus vector, in a macaque AIDS model. J Virol 77: 9710–9715.
41. Kestler HW III, Ringler DJ, Mori K, Panicali DL, Sehgal PK, et al. (1991) Importance of the nef gene for maintenance of high virus loads and for development of AIDS. Cell 65: 651–662.
42. Yamamoto H, Kawada M, Takeda A, Igarashi H, Matano T (2007) Post-infection immunodeficiency virus control by neutralizing antibodies. PLoS One 2: e540.
43. Iwamoto N, Tsukamoto T, Kawada M, Takeda A, Yamamoto H, et al. (2010) Broadening of CD8+ cell responses in vaccine-based simian immunodeficiency virus controllers. AIDS 24: 2777–2787.
44. Voss G, Nick S, Stahl-Hennig C, Ritter K, Hunsmann G (1992) Generation of macaque B lymphoblastoid cell lines with simian Epstein-Barr-like viruses: transformation procedure, characterization of the cell lines and occurrence of simian foamy virus. J Virol Methods 39: 185–195.
45. Kawada M, Igarashi H, Takeda A, Tsukamoto T, Yamamoto H, et al. (2006) Involvement of multiple epitope-specific cytotoxic T-lymphocyte responses in vaccine-based control of simian immunodeficiency virus replication in rhesus macaques. J Virol 80: 1949–1958.
46. Tenzer S, Wee E, Burgevin A, Stewart-Jones G, Friis L, et al. (2009) Antigen processing influences HIV-specific cytotoxic T lymphocyte immunodominance. Nat Immunol 10: 636–646.
47. Ishii H, Kawada M, Tsukamoto T, Yamamoto H, Matsuoka S, et al. (2012) Impact of vaccination on cytotoxic T lymphocyte immunodominance and cooperation against simian immunodeficiency virus replication in rhesus macaques. J Virol 86: 738–745.
48. Flores-Villanueva PO, Yunis EJ, Delgado JC, Vittinghoff E, Buchbinder S, et al. (2001) Control of HIV-1 viremia and protection from AIDS are associated with HLA-Bw4 homozygosity. Proc Natl Acad Sci USA 98: 5140–5145.
49. Martin MP, Gao X, Lee JH, Nelson GW, Detels R, et al. (2002) Epistatic interaction between KIR3DS1 and HLA-B delays the progression to AIDS. Nat Genet 31: 429–434.
50. Martin MP, Qi Y, Gao X, Yamada E, Martin JN, et al. (2007) Innate partnership of HLA-B and KIR3DL1 subtypes against HIV-1. Nat Genet 39: 733–740.

JVI
Journals.ASM.org

No Viral Evolution in the Lymph Nodes of Simian Immunodeficiency Virus-Infected Rhesus Macaques during Combined Antiretroviral Therapy

Megu Oue, Saori Sakabe, Mariko Horiike, Mika Yasui, Tomoyuki Miura, Tatsuhiko Igarashi

Laboratory of Primate Model, Experimental Research Center for Infectious Diseases, Institute for Virus Research, Kyoto University, Kyoto, Japan

To elucidate the mode of viral persistence in primate lentivirus-infected individuals during combination antiretroviral therapy (cART), four simian immunodeficiency virus 239-infected monkeys were treated with cART for 1 year. The viral *env* genes prepared from total RNA extracted from the mesenteric lymph nodes collected at the completion of therapy were assessed by single genome amplification. Analyses of nucleotide substitutions and phylogeny revealed no viral evolution during cART.

Combination antiretroviral therapy (cART) has transformed human immunodeficiency virus (HIV) infection from an incurable disease to a manageable one. It suppresses the viral burden in patients to undetectable levels (1–3), lowers the chance of viral transmission (4), increases the number of $CD4^+$ T lymphocytes (1, 2), reconstitutes immunity (5–7), and extends the life expectancy of patients (8). However, cART does not cure patients because of its inability to eradicate the virus from infected individuals (9), suggesting the existence of a viral reservoir that is refractory to cART. Its identification and eradication are therefore requisites for a functional cure for AIDS. To establish a strategy for eradication of the HIV reservoir, the mechanism of persistence of the virus must be elucidated. Two mechanisms of viral persistence have been proposed: one is ongoing cycles of viral replication despite the presence of antivirals (10), and the other is provirus integration into long-lived cells (11). Whereas previous studies concerning this issue have been extensively conducted with clinical specimens from HIV-1-infected patients, including plasma, peripheral blood mononuclear cells, and gut-associated lymphatic tissues (12–14), lymph nodes, which are epicenters of virus replication in infected individuals not undergoing therapy (15–17), have only rarely been subjected to scrutiny. In animal models of cART, in particular, the simian immunodeficiency virus (SIV)-macaque model, which allows systemic examination, the location of the viral reservoir and the mechanism of viral holding have not been studied in detail.

To elucidate how the virus is maintained during cART in an animal model of anti-HIV chemotherapy, we administered a combination of nucleotide/nucleoside reverse transcriptase inhibitors (azidothymidine, lamivudine, and tenofovir disoproxil fumarate) and protease inhibitors (lopinavir with ritonavir) to four SIV239-infected rhesus macaques for 1 year (18). Although the plasma viral RNA loads of the animals were suppressed to levels below the assay detection limit during the period of chemotherapy, a systemic analysis conducted at the completion of therapy revealed viral RNA present in lymphatic tissues, especially in mesenteric and splenic lymph nodes (MLN and SLN, respectively) at high titers. Reasoning that any possible mode(s) of viral persistence should be in operation in tissues with high levels of viral RNA expression, we investigated viral genes in these tissues.

It is expected that viral genes accumulate nucleotide substitutions in proportion to the time postinfection in individuals not undergoing therapy because of continuous virus replication mediated by the error-prone viral reverse transcriptase. Such mutation rates have indeed been observed in the V3 loop of *env*, p17 of *gag* (19), and the C2-to-C5 region of *env* (20) in HIV-1-infected patients, as well as in the *env* gene from monkeys experimentally infected with SIV (21, 22). We hypothesized that viral genes would accumulate mutations if the virus was continuously replicating in the reservoir despite the presence of antivirals.

First, to ascertain whether such an accumulation of mutations took place at a detectable magnitude in our experimental system, we used SIV239, a molecularly cloned virus, to infect macaques for 1 year and periodically sampled viral genes from the untreated control animal (MM521). To reveal ongoing expression of viral genes at sampling, total RNA was extracted from plasma samples collected at 8, 18, 42, and 68 weeks postinfection (wpi) and examined. Single-genome amplification (SGA) (23) was used to amplify the viral genes present and to avoid the selective amplification of a particular genotype or recombination between genotypes during PCR. Using a nested PCR method, we amplified the entire *env* gene, which accumulates nucleotide substitutions in the greatest numbers, following reverse transcription of cDNA from the extracted RNA. The initial PCR cycles were carried out with the following primers: forward, SIV20F (5′-CTC CAG GAC TAG CAT AAA TGG-3′); reverse, SHenv9R (5′-GGG TAT CTA ACA TAT GCC TC-3′). Successive PCR cycles were run with the following primers: forward, SIV21F (5′-CTC TCT CAG CTA TAC CGC CC-3′); reverse, SHenv8R (5′-GCC TTC TTC CTT TTC TAA G-3′). The PCR products from an average of 12 independent reactions per time point were directly subjected to sequencing.

We computed the number of mutations in each SGA clone obtained from plasma samples of an untreated monkey (MM521) through a comparison with that of the inoculum virus (Fig. 1). A

Received 6 December 2012 Accepted 2 February 2013
Published ahead of print 13 February 2013
Address correspondence to Tatsuhiko Igarashi, tigarash@virus.kyoto-u.ac.jp.
Supplemental material for this article may be found at http://dx.doi.org/10.1128/JVI.03367-12.

doi:10.1128/JVI.03367-12

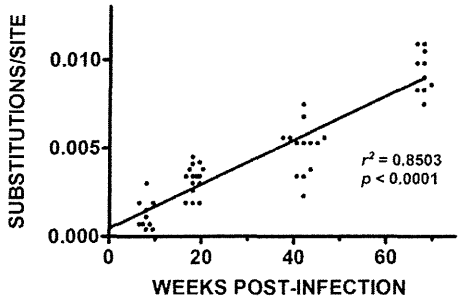

FIG 1 Time-dependent accumulation of nucleotide substitutions in SIV genomes circulating in an infected and untreated rhesus macaque. The sequences of viral *env* genes in circulation collected at 8, 18, 42, and 68 wpi from SIV239-infected animals and an untreated animal (MM521) were determined. Tamura-Nei distances (36) of the sequences were computed with the MEGA5 software (37), and the number of nucleotide substitutions per site was plotted against the number of weeks postinfection. Each symbol represents a single genomic amplicon derived from plasma samples collected at the time points designated.

linear relationship with a coefficient of 1.25×10^{-4} ($r^2 = 0.8503$, $P < 0.0001$; GraphPad Prism, La Jolla, CA) was revealed between the number of mutations in the SGA clones and the time postinfection. By using the coefficient, the cumulative number of mutations per annum was determined to be 6.5×10^{-3} substitutions/site/year, a value comparable to those of SIV and HIV reported previously (9×10^{-3} [21, 22] and 6.0×10^{-3} [23] substitutions/site/year, respectively). The accuracy of the "molecular clock" in our experimental setting prompted us to examine viral RNA extracted from the lymph nodes of animals that underwent cART for 1 year.

Total RNA was extracted from the MLN of four treated animals and one untreated animal, as well as the SLN of one of the treated animals (MM530), at the completion of the observation period and used as the template for PCR; the products were subjected to sequence analysis as described above. On average, 10 sequences were obtained from each sample (Fig. 2A and Table 1). The number of mutations observed in the *env* gene from MM521 (untreated) was, on average, 25 of 2,700 bases. In contrast, the number in treated animals was, on average, 1.5 of 2,700 bases (Table 1). The difference in the number of mutations in *env* between the plasma and MLN samples from the untreated animal, MM521, at 68 wpi (at necropsy) was statistically insignificant ($P > 0.05$; Fig. 2A), justifying our comparison of these two distinct anatomical compartments. Thus, we proceeded to compare the substitution numbers in plasma at 8 wpi, immediately before the onset of cART, with those from the lymph nodes of animals treated with cART at necropsy (61 to 65 wpi). The number of nucleotide substitutions in the *env* gene in both the plasma and MLN of the untreated animal (MM521) at 68 wpi was higher than that in plasma at 8 wpi ($P < 0.0001$). In contrast, those in the MLN of treated animals at the completion of cART were unchanged (MM528 and SLN of MM530) or decreased significantly (MM491, MM499, and MLN of MM530) (Fig. 2A). The results indicated that the virus did not accumulate further mutations beyond those obtained by 8 wpi.

As the samples were collected from animals at various time points postinfection, the numbers depicted in Fig. 2A were converted to substitutions/site/year (Fig. 2B) for further analysis. Comparison of the number of viral mutations in plasma at 8 wpi

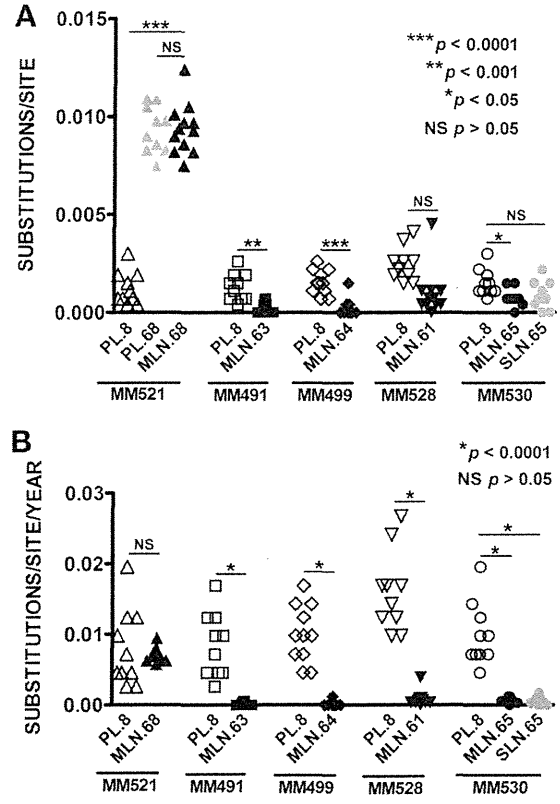

FIG 2 Nucleotide substitutions in *env* genes from SIV239-infected animals. The number of mutations in *env* from the plasma (PL, at 8 and 68 wpi) and MLN (at 68 wpi) of an SIV-infected but untreated animal (MM521) and from the plasma (at 8 wpi) and MLN (at necropsy, 61, 63, 64, or 65 wpi) and SLN (at necropsy, 65 wpi) from SIV-infected and treated monkeys (MM491, MM499, MM528, and MM530) were assessed as described in the legend to Fig. 1. (A) Numbers of nucleotide substitutions per site are shown. The statistical significance of differences between substitution numbers was evaluated by Student's *t* test using GraphPad Prism. *, $P < 0.05$; **, $P < 0.001$; ***, $P < 0.0001$; NS, $P > 0.05$. (B) Numbers of nucleotide substitutions per annum are shown. *, $P < 0.001$; NS, $P > 0.05$.

(median, 5.9×10^{-3} substitutions/site/year) with that in the MLN (median, 7.2×10^{-3} substitutions/site/year) in the untreated animal, MM521, indicated no statistically significant difference ($P = 0.6265$), as predicted by the analysis in Fig. 2A. Next, we compared the numbers in animals that underwent chemotherapy. At 8 wpi, the treated animals were equivalent to MM521 (an untreated animal) in terms of therapeutic status, since cART was started after sample collection at 8 wpi. Not unexpectedly, there was no statistically significant difference in the number of substitutions/site/year in plasma between the untreated and treated animals (MM491, 8.5×10^{-3}; MM499, 9.8×10^{-3}; MM528, 1.6×10^{-2}; MM530, 8.5×10^{-3}; MM521, 5.9×10^{-3}), except for MM528 ($P = 0.0048$ compared to the value for the untreated animal). In contrast, the number of mutations per annum in the lymph nodes of treated animals collected at necropsy (median, 3.4×10^{-4} substitutions/site/year) was significantly lower than that in the plasma of the animals at 8 wpi (median, 9.8×10^{-3} substitutions/site/year; $P < 0.0001$). The number of mutations per year in the lymph nodes also differed significantly between the untreated and treated macaques ($P < 0.0001$). This supports the hypothesis that ongoing viral replication contributed little, if anything, to viral persistence during cART.

TABLE 1 Origins and numbers of *env* clones

Animal (cART) and specimen	Sample collection time (wpi)	No. of SGA clones	No. of nucleotide substitutions	
			Minimum/ maximum	Mean ± SD
MM521 (untreated)				
Plasma	8	10	1/8	3.3 ± 2.2
Plasma	68	10	20/29	24.9 ± 3.2
MLN	68	12	20/33	25.0 ± 3.4
MM491 (treated)				
Plasma	8	10	1/7	3.5 ± 1.8
MLN	63	10	0/2	0.6 ± 0.8
MM499 (treated)				
Plasma	8	11	2/7	4.2 ± 1.7
MLN	64	10	0/4	0.7 ± 1.3
MM528 (treated)				
Plasma	8	10	4/11	6.6 ± 2.4
MLN	61	11	0/3 (12)[a]	1.7 ± 1.1[b]
MM530 (treated)				
Plasma	8	10	2/8	4.0 ± 1.7
MLN	65	10	0/4	2.1 ± 1.2
SLN	65	10	0/6	2.4 ± 1.9

[a] Interpreted as a hypermutant driven by APOBEC3G/F (Hypermut 2.0, http://www.hiv.lanl.gov/content/index).
[b] Computed excluding the clone with hypermutation.

Examination of the nucleotide substitution numbers did not indicate discernible *de novo* virus replication during cART. Therefore, we next investigated continuous viral replication during cART through phylogenetic analysis of viral *env* clones. Clones were obtained from the untreated animal (derived from plasma at 8, 18, 42, and 68 wpi and from MLN) and from one of the treated animals (derived from plasma at 8 wpi and from MLN at necropsy) (Fig. 3; see Fig. S1 in the supplemental material). To illustrate the accumulation and specific sites of mutations, Highlighter plot analysis (http://www.hiv.lanl.gov/content/sequence/HIGHLIGHT/help.html) was also performed. Phylogenetic analysis of the viral genes from the untreated animal revealed that (i) *env* clones from plasma exhibited increasing genetic distance from the inoculum virus with time; (ii) clones obtained at a given time point branched out of the one immediately before, a clear demonstration of viral evolution; and (iii) clones from lymph nodes formed a cluster with those from plasma collected at the same time. In contrast, clones from treated animals, regardless of the tissue origin or time point, formed a cluster with clones derived from the plasma of the untreated animal at 8 wpi and the inoculum virus (Fig. 3; see Fig. S1). The results of the Highlighter plot analysis were consistent with those of the phylogenetic analysis. These results clearly demonstrated that viral evolution did not take place in SIV239-infected rhesus macaques during cART. Analysis of the *env* genes in the peripheral blood

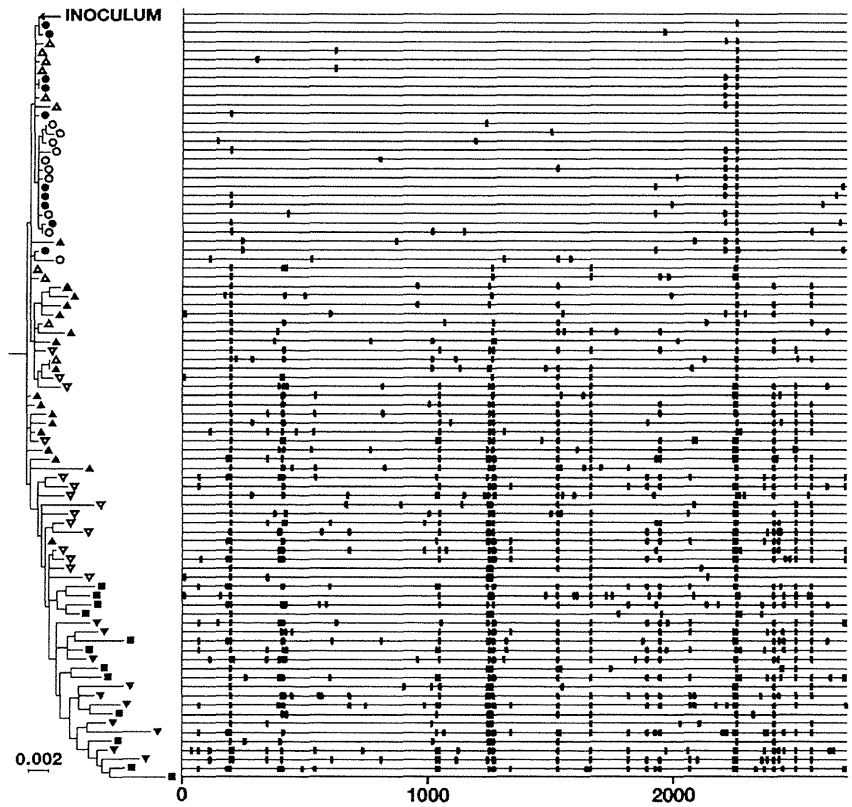

FIG 3 Phylogenetic relationship of *env* sequences from treated (MM530) and untreated (MM521) SIV-infected animals. Sequences of the entire *env* gene from both animals were subjected to phylogenetic analysis. The phylogenetic tree was constructed by the maximum-likelihood method (38). Open circles, sequences in the plasma of MM530 at 8 wpi; closed circles, those from the MLN of MM530 at 65 wpi; open triangles, those from plasma of MM521 at 8 wpi; closed triangles, those from plasma of MM521 at 18 wpi; open inverted triangles, those from plasma of MM521 at 42 wpi; closed inverted triangles, those from plasma of MM521 at 68 wpi; closed rectangles, those from MLN of MM521 at 68 wpi. The scale represents a genetic distance equivalent to 0.002 substitution/site. The corresponding sequence of SIVmac251 32H (GenBank accession no. D01065) was used as the outgroup.